Acta Pharmaceutica Sinica B 2025;15(6):2985−3007

Chinese Pharmaceutical Association
Institute of Materia Medica, Chinese Academy of Medical Sciences

Acta Pharmaceutica Sinica B

www.elsevier.com/locate/apsb
www.sciencedirect.com

REVIEW

Unravelling the target landscape of tranylcypromines for new drug discovery

Yihui Song[a,e], Junbiao Chang[d,*], Bin Yu[b,c,d,*]

[a]*School of Pharmaceutical Sciences, Zhengzhou University, Zhengzhou 450001, China*
[b]*Tianjian Laboratory of Advanced Biomedical Sciences, Institute of Advanced Biomedical Sciences, Zhengzhou University, Zhengzhou 450001, China*
[c]*State Key Laboratory of Metabolic Dysregulation & Prevention and Treatment of Esophageal Cancer, College of Chemistry, Zhengzhou University, Zhengzhou 450001, China*
[d]*College of Chemistry, Pingyuan Laboratory, Zhengzhou University, Zhengzhou 450001, China*
[e]*Key Laboratory of Gastrointestinal Cancer (Fujian Medical University), Ministry of Education, Fujian Medical University, Fuzhou 350122, China*

Received 12 September 2024; received in revised form 1 April 2025; accepted 2 April 2025

KEY WORDS

Tranylcypromine;
Privileged scaffold;
Target space;
New drug discovery;
Amine oxidase;
Platelet $P2Y_{12}$ receptor;
Cytochrome P450 superfamily;
Human immunodeficiency virus type 1

Abstract Molecular editing around privileged scaffolds, also known as periphery editing, is a commonly used strategy in contemporary drug discovery and development. Tranylcypromine (TCP) is a widely acknowledged scaffold with diverse pharmacological activities. TCP-derived compounds target different enzymes and cellular receptors such as amine oxidase, platelet $P2Y_{12}$ receptor, and cytochrome P450 superfamily. These compounds have demonstrated various effects including antidepressant, anticancer, antiviral properties, involvement in prostaglandin synthesis, and mediation of drug metabolism. Notably, the first reversible oral $P2Y_{12}$ receptor antagonist, ticagrelor, is currently used to prevent future myocardial infarction, stroke, and cardiovascular death. Several TCP-based lysine demethylase 1 (LSD1) inhibitors are currently undergoing clinical assessment. MIV-150, a third-generation non-nucleoside reverse transcriptase inhibitor, has progressed to the clinical stage for treating human immunodeficiency virus type 1 (HIV-1) seronegative patients suffering from acute coronary syndrome. This review aims to explore the target landscape of TCPs, highlight key structure−activity relationships (SARs), and emphasize the therapeutic potential of TCPs for treating various diseases. Finally, the lessons learned from our medicinal chemistry practice, challenges and future directions of TCP-based drug discovery are briefly discussed.

*Corresponding authors.
E-mail addresses: changjunbiao@zzu.edu.cn (Junbiao Chang), zzuyubin@hotmail.com (Bin Yu).

Peer review under the responsibility of Chinese Pharmaceutical Association and Institute of Materia Medica, Chinese Academy of Medical Sciences.

https://doi.org/10.1016/j.apsb.2025.04.012

1. Introduction

The concept of "privileged scaffold" was originally introduced by Evans and his colleagues in the late 1980s, defining it as "structures motifs capable of providing high-affinity ligands for multiple biological targets"[1]. Modifying privileged scaffolds is a widely used strategy for lead generation[1]. Constructing structurally unique and diverse bioactive compound collections based on the privileged scaffolds can dramatically speed the drug discovery process[2].

Tranylcypromine, alternatively known as *trans*-2-phenylcyclopropylamine, TCP and 2-PCPA, has been recognized as a privileged scaffold for designing novel chemotypes with significant pharmacological activities. TCP can regulate the neurotransmitter level by targeting monoamine oxidases (MAOs). Thereby, it has been approved as an antidepressant drug for the treatment of patients with major depressive disorder[3]. Beyond its role as an antidepressant, TCP derivatives also exhibit a wide spectrum of biological functions (*e.g.*, anti-cancer, anti-inflammatory, prostaglandin synthesis, and drug metabolism) by inhibiting various enzymes such as histone lysine demethylases (LSDs), the cytochrome P450 (CYPs) superfamily, cellular receptor and other enzymes (Fig. 1)[4–9]. Molecular editing around the TCP structure has led to designing compounds with therapeutic promise. The strategies for synthesizing TCP and its derivatives primarily involve direct synthesis from cyclopropane-based intermediates and the *de novo* construction of cyclopropane structures, such as through the Corey−Chaykovsky reaction and Kulinkovich-de Meijere reaction[10]. Notably, several lysine demethylase 1 (LSD1)-targeted compounds designed based on the TCP scaffold (*e.g.*, ORY-2001, ORY-1001, and TAK-418) have advanced into clinical trials as either mono- or combinational therapy[5,11]. The $P2Y_{12}$ receptor antagonist ticagrelor has been approved for reducing the risk of heart attack, stroke, or death in patients suffering from acute coronary syndrome (ACS)[6]. Besides, MIV-150, a human immunodeficiency virus type 1 (HIV-1) reverse transcriptase inhibitor, also has entered clinical trials to evaluate its safety and pharmacokinetics for HIV-1 seronegative patients[12]. Collectively, the distinctive structural features of TCP, coupled with its diverse biological activities, have made TCP a privileged scaffold for new drug discovery.

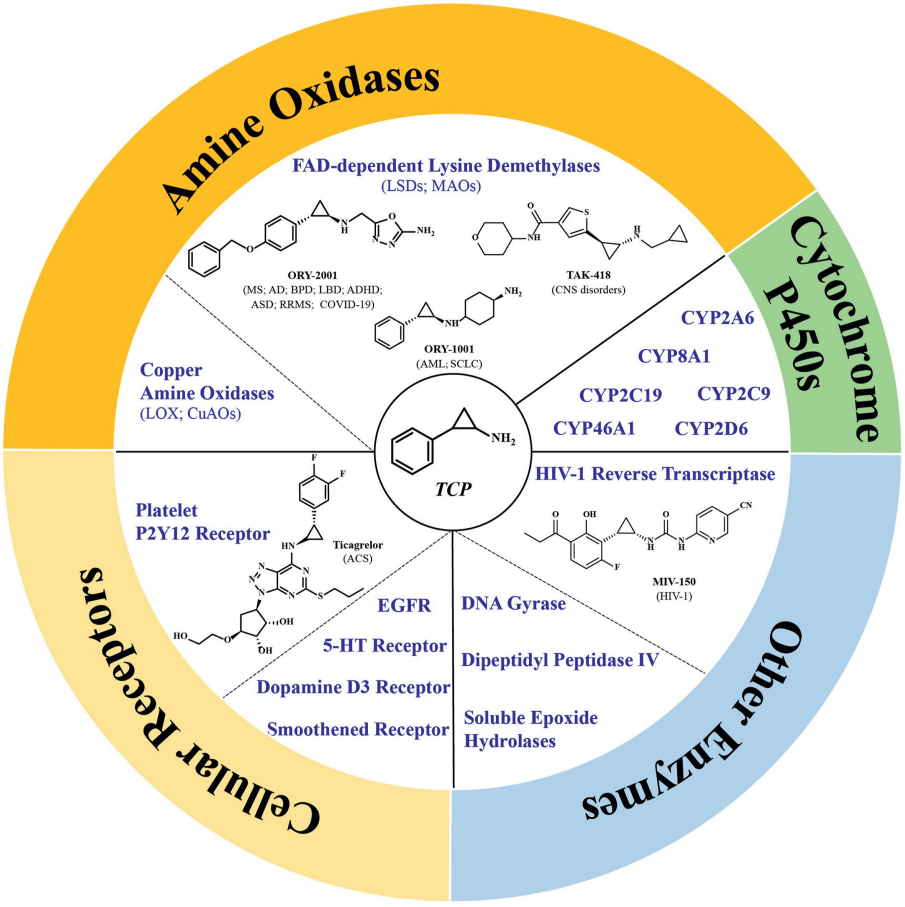

Figure 1 The drug target landscape of TCP derivatives.

In this review, we aim to highlight advancements of TCPs in drug discovery and to reveal their drug landscape. The primary structure−activity relationships (SARs), key binding modes of TCP analogs, therapeutic potential against various diseases, and challenges of TCP analogs across different targets are discussed. Furthermore, we also share our lessons learned from our medicinal chemistry practice towards the development of LSD1 inhibitors and comment on the challenges and future directions of TCP-based new drug discovery campaigns.

2. Drug discovery targeting amine oxidases

Amine oxidases (AOs), including flavin adenine dinucleotide (FAD)-dependent amine oxidases (FAOs) and copper amine oxidases (CuAOs), play integral roles in the biotransformation of aminergic neurotransmitters (*e.g.*, catecholamines, histamine, and serotonin), as well as the detoxification of toxins and carcinogens in foods and the environment[13,14]. AOs are essential in the regulation of neurotransmitter amines levels, such as dopamine (DA), catecholamines norepinephrine (NE), and the indolealkylamine 5-hydroxytryptamine (5-HT, serotonin), which are pivotal in maintaining both homeostatic and xenobiotic metabolic pathways[4,13]. TCP analogs are covalent regulators of AOs and exhibit a wide range of biological activities, underscoring the biological significance of the TCP scaffold in drug discovery targeting AOs.

2.1. FAD-dependent amine oxidases

The FAOs family shares conserved catalytic mechanism, namely the cyclopropyl ring of TCP covalently modifies the flavin adenine dinucleotide (FAD) cofactor within the catalytically active site *via* the single-electron transfer mechanism, subsequently leading to the open of cyclopropyl ring[15]. Three possible pathways are (Fig. 2): (1) A cyclic adduct is initially formed, and then the bond is opened to either the N_5 or C_{4a} atoms preferentially depending on the chirality of the cyclopropyl groups; (2) A single-linkage adduct is initially formed, subsequently the group that attaches to the flavin is either chemically recombined or migrated[16]. *Via* forming five types of TCP-FAD adducts, including five-membered ring adduct, C_{4a} adduct, N_5 adduct A, N_5 adduct B, and F-FAD adduct, the demethylase activity of LSD1 is suppressed. The five-membered ring adduct and C_{4a} adduct can be produced followed by two different cleavages of the cyclopropyl ring[17]. In pathway A, the opening of cyclopropyl ring results in the forming of an imine intermediate and a benzylic carbon radical, followed by an interaction between the benzylic radical of TCP and C_{4a} of FAD. Subsequently, a five-membered ring adduct linking C_{4a} and N_5 of FAD is produced after the amine and cyclization hydrolysis process[17]. Additionally, the five-membered ring adduct may also serve as an intermediate for the formation of a compact formylated-FAD adduct[18]. In pathway B, the cyclopropyl ring opening leads to the formation of an energetically unfavorable primary carbon radical. The bond formation between primary carbon in TCP and C_{4a} of FAD gives a C_{4a} adduct[17]. Moreover, different enantiomers can also react with FAD to produce different covalent adducts through distinct mechanisms, resulting in varied selectivity and potency. (3) In pathway C, two N_5 adducts that link the ring-opened TCP *via* the N_5 atom of FAD, namely N_5 adduct A and N_5 adduct B, are also identified[19,20]. Compared to MAOs, the wider space at position 4 of the phenyl ring in LSD1's TCP-FAD adduct allows for accommodating substituents of various sizes when designing selective LSD1 inhibitors[21].

Based on the single-electron transfer mechanisms illustrated in Fig. 2, we propose that dialkylation (especially with steric groups) or acylation of the TCP amine group could notably reduce the inhibitory potency. These crucial SAR trends have been observed in our medicinal chemistry efforts aimed at designing LSD1 inhibitors. The introduction of such groups may impact the generation and transfer of single electrons, which is a crucial factor for medicinal chemists to consider when designing inhibitors for FAD-dependent amine oxidases[22]. Fully understanding the covalent binding mechanisms of various TCPs against FAD-dependent amine oxidases will aid in the design of potent and selective inhibitors.

The MAOs and LSDs belong to the well-defined FAOs family with substrate specificities[23]. TCP acts as a nonselective and irreversible MAOs inhibitor, consequently raising neurotransmitter levels in the brain by impeding the catabolism of serotonin and norepinephrine[12,24]. In consideration of the high structural homology among FAOs, TCP has been repurposed as an anticancer agent targeting LSDs[25]. Using TCP as a privileged scaffold, significant advancements have been made in the LSDs-targeted drug discovery[25].

2.1.1. FAD-dependent lysine demethylases

LSDs comprise two members LSD1 and LSD2[26]. The LSDs family features a conserved SWI3/Rsc8/Moira (SWIRM) domain (24% sequence identity) and an amine oxidase domain (AOD). Nonetheless, the overall architectural structures of LSDs are notably distinct (Fig. 3A)[27]. Both LSD1 and LSD2 use a shared catalytic demethylase mechanism to remove methyl marks from mono- or di-methylated histone H3 lysine 4 and 9 (H3K4/9), with FAD serving as a cofactor[26]. The distinct domain architectures of LSDs, such as the Tower domain in LSD1 and the zinc-finger domain in LSD2, enable them to engage with diverse binding partners, thus manifesting different biochemical characterization (Fig. 3A)[28]. LSDs play pivotal roles in numerous cellular processes, underlining their therapeutic potential for treating various diseases[29]. In contrast to the interior cavities of MAOs (MAO-A PDB code: 2BXR; MAO-B PDB code: 2BYB) gated by surface loops, LSDs (LSD1 PDB code: 2H94, 2HKO and 2Z3Y; LSD2 PDB code: 4FWE, 4FWJ and 4UGI) feature much open and hydrophobic clefts that accommodate substrates *via* specific interaction networks. The substantial variations in the architectures of the substrate binding sites within the FAOs favor the development of highly potent and selective inhibitors[20].

Structural overlapping of TCP in complexes with LSD1 (PDB code: 2EJR) and LSD2 (PDB code: 4GUU) showed that the covalent TCP-FAD adducts resided within the hydrophobic pockets composited by residues His564/Asn440, Thr335/Val439, Ala539/Ala546, Phe538/Tyr545, Tyr761/Tyr767, Thr810/Val805 and Thr335/Val439. The phenyl ring of the adduct was located in the active site cavities of LSDs, making weak *van der waals* contacts with the surrounding residues (Fig. 3B and C)[19,30]. Due to the orbital changes of flavin atoms, the crucial water-mediated hydrogen bond interaction between the flavin N_5 atom and the conserved residue Lys661 was disrupted, compared to the apo-LSDs. Thereby, the process involving electron and proton transfer was impeded, leading to inhibition of LSDs[19,30]. The main covalent adducts found in the reaction between LSDs and TCP are a five-membered ring model, as seen in the crystal structures of the LSD1/CoREST/TCP complex (PDB code: 2UXX) and LSD2/NPAC/TCP complex (PDB code: 4GUU)[17,30]. Additionally, altering the configuration of one chiral center also affected the

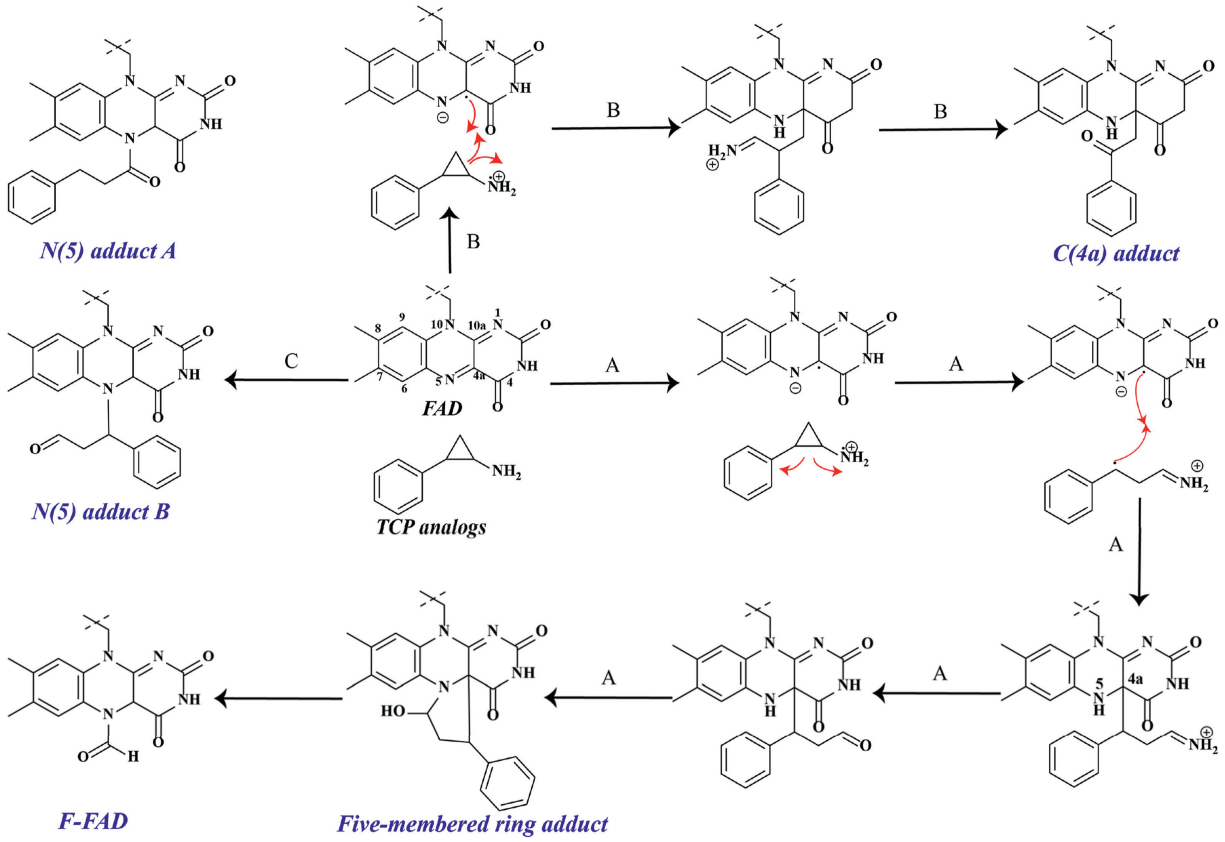

Figure 2 Covalent binding mechanisms of TCPs against FAD-dependent amine oxidases.

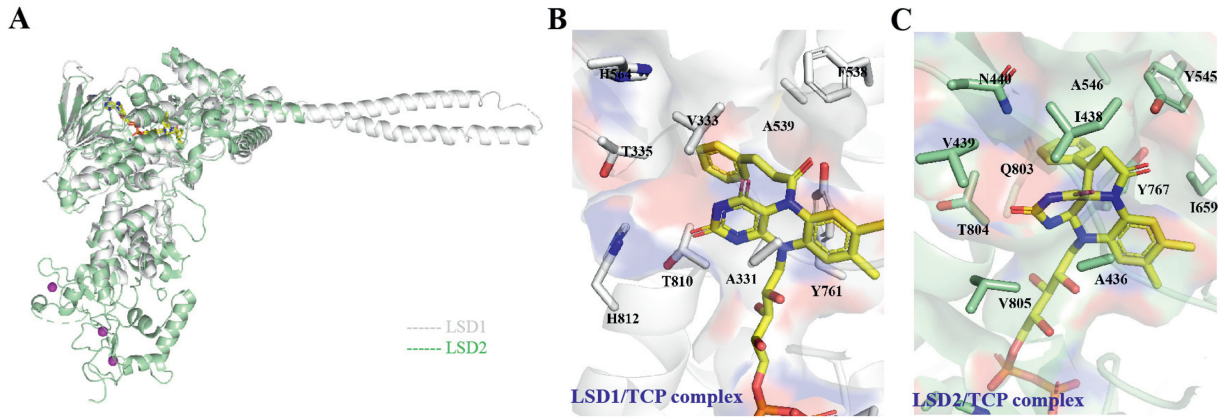

Figure 3 Structural features of LSDs and the binding mode of TCP with LSDs. (A) Structural overlapping of LSD1 (white cartoon) and LSD2 (palegreen cartoon). FAD: yellow sticks. Zinc: magentas ball. (B, C) The binding mode of TCP in complex with LSD1 (B, PDB code: 2EJR) and LSD2 (C, PDB code: 4GUU). FAD-TCP adduct: yellow sticks.

orientation of the phenyl ring and its covalent linkage with the flavin N_5 atom. This likely occurred through different mechanistic pathways. Both N_5 adduct A and N_5 adduct B were observed in the crystal structure of the LSD1/TCP complex solved at 2.25 Å (PDB code: 2EJR), as well as in LSD1/chiral TCPs complexes[19,20]. The structure of the LSD1/(−)-*t*PCPA complex (PDB code: 2EJR) revealed the presence of N_5 adduct A. In this case, the phenyl ring of (−)-*t*PCPA (LSD1 K_i = 168 μmol/L; LSD2 K_i = 127 μmol/L) was positioned at the core of substrate binding pocket, directly above the flavin ring. Conversely, the phenyl ring of (+)-*t*PCPA (LSD1 K_i = 284 μmol/L; LSD2 K_i = 137 μmol/L) was situated within a lateral cavity of the substrate binding pocket away from the flavin ring. The configuration of the N_5 adduct B in the LSD1/(+)-*t*PCPA complex was modeled (PDB code: 2XAH)[20]. These differences may account for the stronger inhibition of (−)-*t*PCPA against LSD1 compared to its enantiomer[20].

The notably spacious substrate binding pocket in LSDs, as opposed to MAOs, favors the development of highly potent and selective TCP-based inhibitors against LSDs by fulfilling the unfilled areas[31,32]. TCP modifications are primarily focused on the

phenyl ring and the amine group to improve the selectivity and potency[22,25,33], whereas modifications on the cyclopropyl core of TCP are relatively rare, probably because of the synthetic intractability and inherent stereochemistry of the TCP core structure. Conformationally constrained TCPs have also been developed, given that two enantiomers of TCP exhibit variations in binding orientation and the conformation of the covalent adduct with FAD[25]. A common structural feature of TCP-based inhibitors is the attachment of the phenyl ring and the amine group to adjacent carbons of the cyclopropyl core, which plays essential roles in adduct complex formation at the active sites. Modifications of the phenyl ring, the amine group or the cyclopropyl core are crucial to the selectivity and potency of TCP analogs against LSD1[22,25,33]. Since 2014, three clinical trials have been launched to evaluate the safety, efficacy, and maximum tolerated dose (MTD) of TCP, either as a standalone treatment or in combination with all-*trans*-retinoic acid (ATRA) and cytarabine (Ara-C), in patients with myelodysplastic syndromes (MDS) and acute myeloid leukemia (AML) (ClinicalTrials.gov identifier: NCT02261779; NCT02273102; NCT02717884) (Table 1)[5,34,35]. To date, TCP-based LSD1 inhibitors, such as GSK-2879552, ORY-1001, ORY-2001, INCB059872, IMG-7289, TAK-418, and LH-1802, have advanced into clinical trials as mono- or combinational therapy (Table 1)[5,11,34].

The binding mode of LSD1/TCP (PDB code: 2EJR) revealed that introducing hydrophobic substituents into the phenyl ring could enhance the potency against LSD1 by facilitating additional interactions with the surrounding hydrophobic residues (Fig. 4A)[19]. The halogenated compound **1** (LSD1 K_i = 3.7 μmol/L) demonstrated a 1000-fold increase in potency against LSDs compared to TCP. This increase was attributed to improved cell permeability and lipophilicity. Notably, both enantiomers of 4-bromophenyl substituted **1** exhibited similar LSD1 inhibitory activity, indicating that changing the stereochemistry of the chiral center had only a subtle effect on their potency[20]. In LSD1/(−)-*trans*-**1** (PDB code: 2XAG) and LSD1/(+)-*cis*-**1** (PDB code: 2XAF) complexes, both enantiomer of **1** adopted a similar N_5 configuration as observed in the LSD1/(−)-*t*PCPA (PDB code: 2EJR)[20]. However, for LSD2, two enantiomers of **1** adopted different covalent configurations, with the orientation of the phenyl ring pointing in different directions. In LSD2/(+)-*cis*-**1** complex (PDB code: 7XE1), the phenyl ring of (±)-*cis*-**1** (LSD1 K_i = 5.9 μmol/L; LSD2 K_i = 80 μmol/L) was pointed towards the catalytic pocket of LSD2, resulting in a similar N_5 adduct as observed in LSD1. In contrast, a C_{4a} covalent adduct with FAD was observed, and the phenyl ring of *trans*-**1** (LSD1 K_i = 2.9 μmol/L; LSD2 K_i = 740 μmol/L) adopted a lateral direction in LSD2/(±)-*trans*-**1** complex (PDB code: 7XE2)[36]. In addition, fluorinated TCP derivatives, such as 2-PFPA (LSD1 IC_{50} = 8.9 μmol/L; LSD1 K_i = 17 μmol/L; MAO-A IC_{50} > 250 μmol/L; MAO-B IC_{50} = 8.3 μmol/L) and S2101 (LSD1 K_i = 0.88 μmol/L; MAO-A IC_{50} = 110 μmol/L; MAO-B IC_{50} = 17 μmol/L), displayed increased inhibitory activity and selectivity against LSD1 compared to TCP. This improvement may be attributed to form different covalent adducts with FAD[37]. The five-membered ring adducts were identified in the LSD1/2-PFPA (PDB code: 3ABT) complexes. In contrast, the crystal structure analysis of LSD1/S2101 complex (PDB code: 6KGL) showed that S2101 was fused to FAD by forming a N_5 adduct A derivative (Fig. 4B)[37]. The enhanced potency of fluorinated TCP derivatives may be explained by the increased stability of FAD-inhibitor adducts, resulting from interactions with surrounding residues in LSD1 (*e.g.*, Ala330, Met332, and Lys661).

Compounds **2** (LSD1 K_i = 1.1 μmol/L; LSD2 K_i = 61 μmol/L; MAO-A K_i = 2.3 μmol/L; MAO-B K_i = 3.5 μmol/L) and **3** (LSD1 K_i = 1.3 μmol/L; LSD2 K_i = 38 μmol/L; MAO-A K_i = 1.2 μmol/L; MAO-B: no inhibition), featuring large hydrophobic substituents, also displayed enhanced potency and selectivity against LSD1 over LSD2 and MAOs[20]. Co−crystal structures of LSD1 in complex with **2** (PDB code: 2XAQ) and **3** (PDB code: 2XAS) revealed that these compounds, acting as plugs, fulfilled the substrate binding cleft of LSD1. In both compounds, the phenyl cyclopropyl groups adopted a similar configuration as that in (−)-*t*PCPA. The bulky chains extended towards the orthogonal orientation of the flavin ring, forming covalent bonds with the flavin N_5 atom of FAD[20]. N_5 adduct A derivatives, similar to that in LSD1/S2101 complex, were observed in both complexes (Fig. 4B). Two conserved hydrogen bonds were observed between the adducts and the crucial residues Lys661 and Asp555 in LSD1[20]. Notably, compared with **2**, the "branched" structure of **3** occupied more areas, with one of the aromatic rings partly protruding out of the binding pocket. These observations may account for the inhibitory activity of both compounds and the significantly higher selectivity of **3** against LSDs over MAOs[20].

N-Alkylated TCP derivatives also demonstrated enhanced potency and improved selectivity (Fig. 5A). Among them, several orally active, potent, and selective LSD1 inhibitors, such as ORY-1001, GSK2879552, TAK-418, ORY-2001, and IMG-7289 have advanced into clinical trials for cancer therapy (Table 1)[22,33,38]. ORY-1001 displayed remarkable potency against LSD1 with IC_{50} value of 18 nmol/L and 1000-fold selectivity over MAOs and LSD2[39]. Mass spectrometry confirmed the presence of both the five-membered ring and N_5 adduct A models in the LSD1/ORY-1001 complex (Fig. 5B). GSK2879552 (LSD1 K_i = 1.7 μmol/L, >280 fold selectivity over other FAD-dependent enzymes) and GSK2699537 were irreversible LSD1 inhibitors developed by GlaxoSmithKline[40]. Similar to other TCP derivatives, GSK-2879552 also formed a covalent bond with the flavin N_5 atom. In contrast, the FAD-GSK2699537 adduct adopted a C_{4a} configuration (Fig. 5B)[40,41]. LSD1/GSK2699537 complex (PDB code undisclosed) revealed hydrogen bond interactions facilitated by the aldehyde group in the FAD-GSK2699537 adduct and residues Ala539 and Ala809 in LSD1[40,42]. The LSD1/GSK2879552 complex (PDB code: 6NQU) showed that additional *N*-substituted groups of GSK2879552 led to new hydrogen bond mediated by residues Val333, Gly330 and Val811, along with hydrophobic interactions with residues Thr335, Val333, Phe538 and Tyr761 in the surrounding extensive spaces (Fig. 6A). These additional interactions may result in the enhanced inhibition and increased selectivity against LSD1 over MAOs[43]. TAK-418 was a TCP analog with lower risk of hematological side effects developed by Takeda. It can inhibit the demethylase activity of LSD1 (IC_{50} = 2.9 nmol/L) while disrupting the interaction between LSD1 and growth factor independent 1B transcriptional repressor (GFI1B)[18]. In the structure of LSD1 in complex with TAK-418 (PDB code: 7E0G), a compact formylated-FAD (F-FAD) covalent adduct with no extra interaction with LSD1 was observed (Fig. 5B and 6B). In contrast, the carbonyl carbon of its (1*S*, 2*S*)-enantiomer covalently bound to the C4 atom in FAD to form an N_5 adduct A (Fig. 5B)[18]. The thiophene ring, substituted with the bulky tetrahydropyranyl amide group in FAD-TAK-418 (1*S*, 2*S*)-enantiomer adduct, may cause steric hindrance with GFI1B, thereby disrupting the interaction between LSD1 and GFI1B[11]. T-3775440 containing a cyclopropylamine moiety also exhibited high potency and selectivity to LSD1 over MAOs

Table 1 TCP-based clinical candidates.

Drug name	Combined therapy	Indication	Trial number	Clinical trial status
TCP 	ATRA	Acute myeloid leukemia	NCT02261779; EudraCT 2012-002154-23	Phase I/II
	ATRA and AraC		NCT02717884	Phase I/II
	ATRA	Myelodysplastic syndromes	NCT02273102	Phase I
	ATRA and AraC		NCT02717884	Phase I/II
ORY-1001 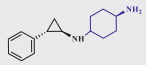	Alone	Small cell lung carcinoma	NCT02913443	Phase I
	Alone	Relapsed/Refractory acute myeloid leukemia	EudraCT 2013-002447-29	Phase I
	Azacitidine		EudraCT 2018-000482-36	Phase IIa
	Platinum-etoposide	Relapsed, extensive-stage disease small cell lung cancer	EudraCT 2018-000469-35	Phase II
GSK2879552 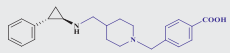	Alone or Azacitidine	Myelodysplastic syndromes	NCT02929498; EudraCT 2016-002294-35	Phase I/II terminated
	Alone	Relapsed/Refractory small cell lung carcinoma	NCT02034123	Phase I terminated
	Alone or ATRA	Acute myeloid leukemia	NCT02177812	Phase I terminated
INCB059872 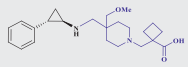	Azacitadine; ATRA; Nivolumab	Advanced malignancies	NCT02712905	Phase I/II
	Alone	Sickle cell disease	NCT03132324	Phase I terminated
	Alone	Relapsed or refractory ewing sarcoma	NCT03514407; EudraCT 2018-000062-11	Phase Ib terminated
	Pembrolizumab; Epacadostat; INCB057643	Advanced solid tumors	NCT02959437	Phase I/II terminated
	Alone	Advanced malignancies	EudraCT 2017-001710-28	Phase I/II terminated
ORY-2001 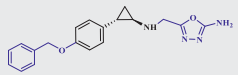	Alone	Alzheimer's disease	NCT03867253; EudraCT 2017-004893-32	Phase IIa
	Alone	Borderline personality disorder	NCT04932291; EudraCT 2021-000350-26	Phase IIb
	Alone	Multiple sclerosis	EudraCT 2017-002838-23	Phase IIa
	Alone	Attention deficit hyperactivity disorder	EudraCT 2018-002140-88	Phase IIa
	Alone	Alzheimer's disease	EudraCT 2019-001436-54	Phase IIa
	Standard of care treatment	Acute respiratory distress syndrome	EudraCT 2020-001618-39	Phase II
IMG-7289 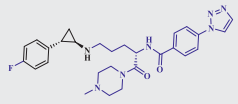	Alone	Essential thrombocythemia	NCT04081220	Phase II
	Alone		NCT04254978; EudraCT 2019-003659-13	Phase IIb
	Alone	Polycythemia vera	NCT04262141	Phase II
	Alone	Myeloproliferative neoplasms	NCT05223920; EudraCT 2021-002452-37	Phase II
	Alone or ATRA	Acute myeloid leukemia Myelodysplastic syndromes	NCT02842827	Phase I/II completed
	Alone	Myelofibrosis	NCT03136185; EudraCT 2018-003811-23	Phase I/II
	Atezolizumab	Extensive stage small cell lung cancer	NCT05191797	Phase I/II
TAK-418 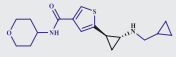	Alone	Normal healthy subject	NCT03228433	Phase I
	Alone		NCT04202497	Phase I
	Alone	Healthy female participants	NCT03501069	Phase I
LH-1802 (structure undisclosed)	Alone	Relapsed or refractory acute myeloid leukemia or myelodysplastic syndrome	CTR20222026	Phase I

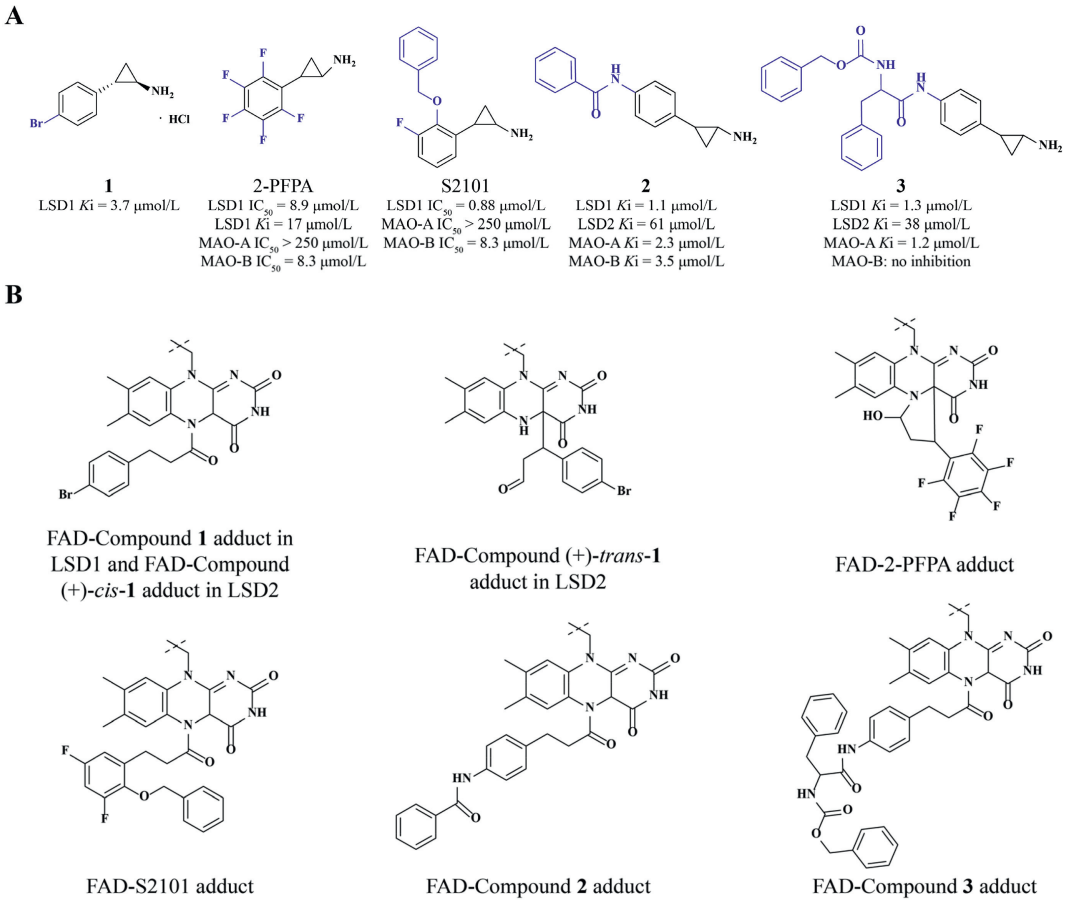

Figure 4 The chemical structures (A) and adducts (B) of representative phenyl-modified TCP derivatives.

(LSD1 IC_{50} = 2.1 nmol/L)[44]. Similar to other TCP analogs, T-3775440 bound to FAD *via* forming a covalent adduct, which may disrupt the interaction between LSD1 and GFI1B−containing complex[44].

The cyclopropane core facilitates the covalent interaction between the catalytic domain of AOs proteins and the inhibitor. In terms of the relatively larger catalytic domain of LSD1 compared to MAO isoforms, introducing hydrophobic groups (*e.g.*, alkyl, phenyl, and benzyl) or larger functional groups at the α- or β-position of cyclopropane ring can significantly enhance the inhibitory activity and selectivity against LSD1 over MAOs (Fig. 7A)[33]. The SARs studies indicated that introducing bulkier substituents at the α-position of cyclopropylamine ring increased the selectivity against LSD1 over MAO-B and to a lesser extent over MAO-A. This could be attributed to the much larger active pockets of LSD1 than MAOs[16]. Crystal structure analysis revealed that (1*R*, 2*S*)-enantiomers **4** and **5** (**4**: LSD1 IC_{50} = 1.78 μmol/L; MAO-A IC_{50} = 1.28 μmol/L; MAO-B IC_{50} = 0.998 μmol/L; **5**: LSD1 IC_{50} = 0.335 μmol/L; MAO-A IC_{50} = 2.59 μmol/L; MAO-B IC_{50} = 28.1 μmol/L) and (1*S*, 2*R*)-enantiomers **6**−**7** (**6**: LSD1 IC_{50} = 3.26 μmol/L; MAO-A IC_{50} = 0.07 μmol/L; MAO-B IC_{50} = 0.007 μmol/L; **7**: LSD1 IC_{50} = 0.131 μmol/L; MAO-A IC_{50} = 0.094 μmol/L; MAO-B IC_{50} = 11.5 μmol/L) adopted different adduct models[16]. The C_{4a} adducts were identified in the complex of LSD1/(1*R*, 2*S*)-enantiomers **4**−**5** (Fig. 7B). In comparison with (1*R*, 2*S*)-analog **4**, (1*S*, 2*R*)-isomer **6** displayed 20- and 140-fold higher potency against MAO-A and MAO-B, respectively, while maintaining only minor inhibitory activity for LSD1. A five-membered cyclic adduct was modelled in the LSD1/**6** complex (Fig. 7B)[16]. Compound **7** with α-phenyl substituent formed an N_5 adduct characterized by a covalent linkage between the flavin N_5 and C1 of the ring-opened **7** (Fig. 7B).

Modification of the cyclopropane, exampled by ethyl-substituted **8** (LSD1 IC_{50} = 0.031 μmol/L) and β-fluorinated **9** (LSD1 IC_{50} = 0.8 μmol/L), led to a significant enhancement of the inhibitory activity against LSD1[45,46]. Additionally, the configuration of TCP derivatives can also affect their inhibitory activity against LSD1[47,48]. Although the absolute configuration of these compounds has minimal effect on LSD1 inhibitory activity, structural changes on the amino group and the benzene ring may favor the potency and selectivity (Fig. 7C)[47]. The simple spirocyclic TCP derivatives compound **10** (LSD1 IC_{50} = 0.17 μmol/L; MAO-A IC_{50} > 100 μmol/L; MAO-B IC_{50} = 0.9 μmol/L) showed 129-fold enhanced LSD1 inhibitory activity compared to that of TCP, while the selectivity against LSD1 over MAO-B was moderate[47]. Further incorporation of substituted benzyl groups to the amino group, exemplified by compounds **11** and **12** (LSD1 IC_{50} < 10 nmol/L), resulted in excellent selectivity profiles against LSD2 and MAOs (>500 fold)[47]. Additionally, compound **13** (LSD1 IC_{50} = 2.2 nmol/L), with conformationally constrained ring systems and the amino-cyclohexane moiety, also displayed good potency and selectivity (>10,000-fold) against LSD1 over MAOs[48].

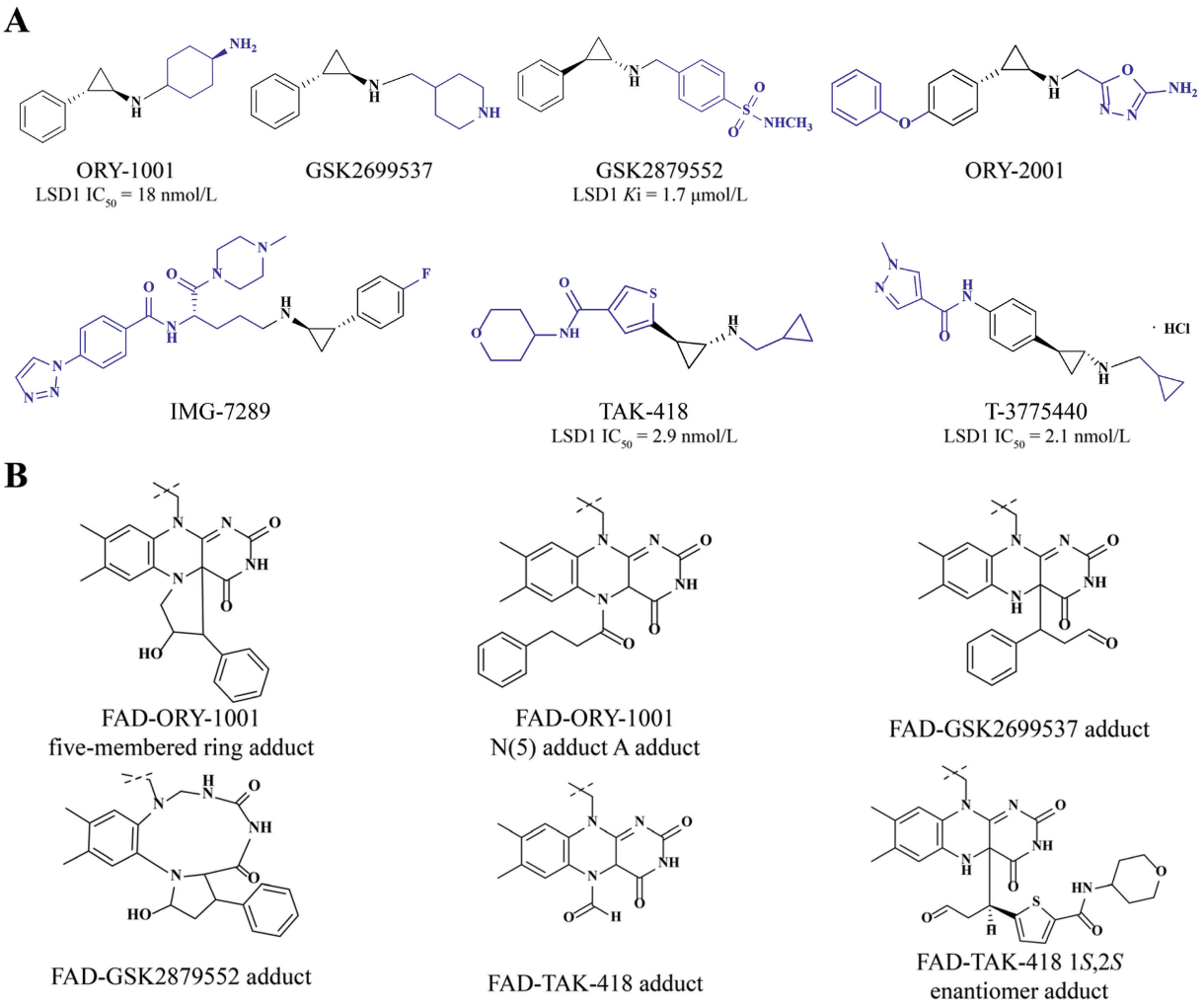

Figure 5 Chemical structures (A) and adducts (B) of representative *N*-alkylated TCP derivatives.

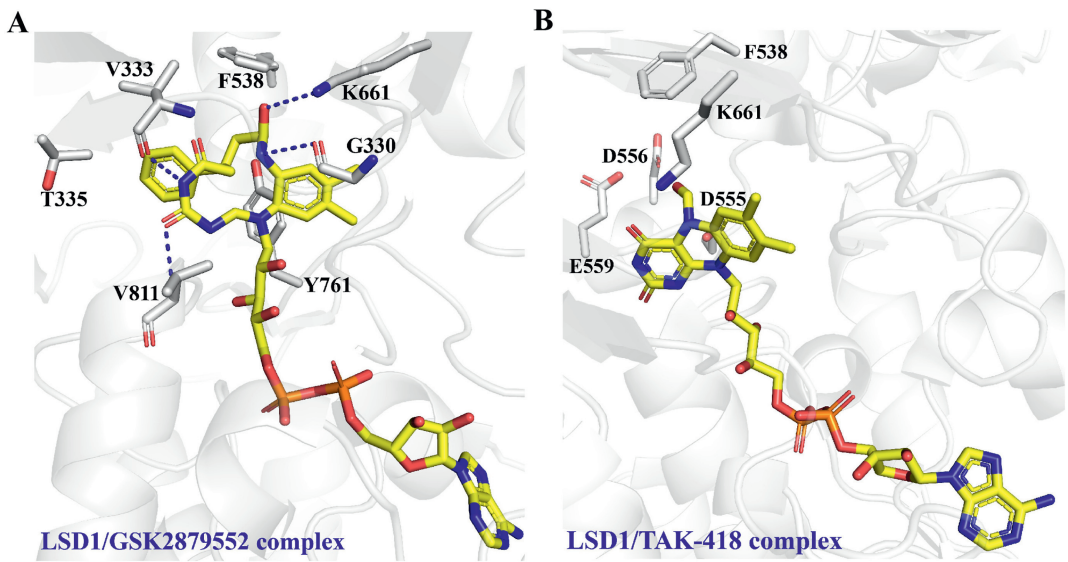

Figure 6 The binding mode of LSD1 in complex with GSK2879552 (A, PDB code: 6NQU) and TAK-418 (B, PDB code: 7E0G). LSD1: white cartoon. FAD-adducts: yellow sticks. Hydrogen bond: blue dotted lines.

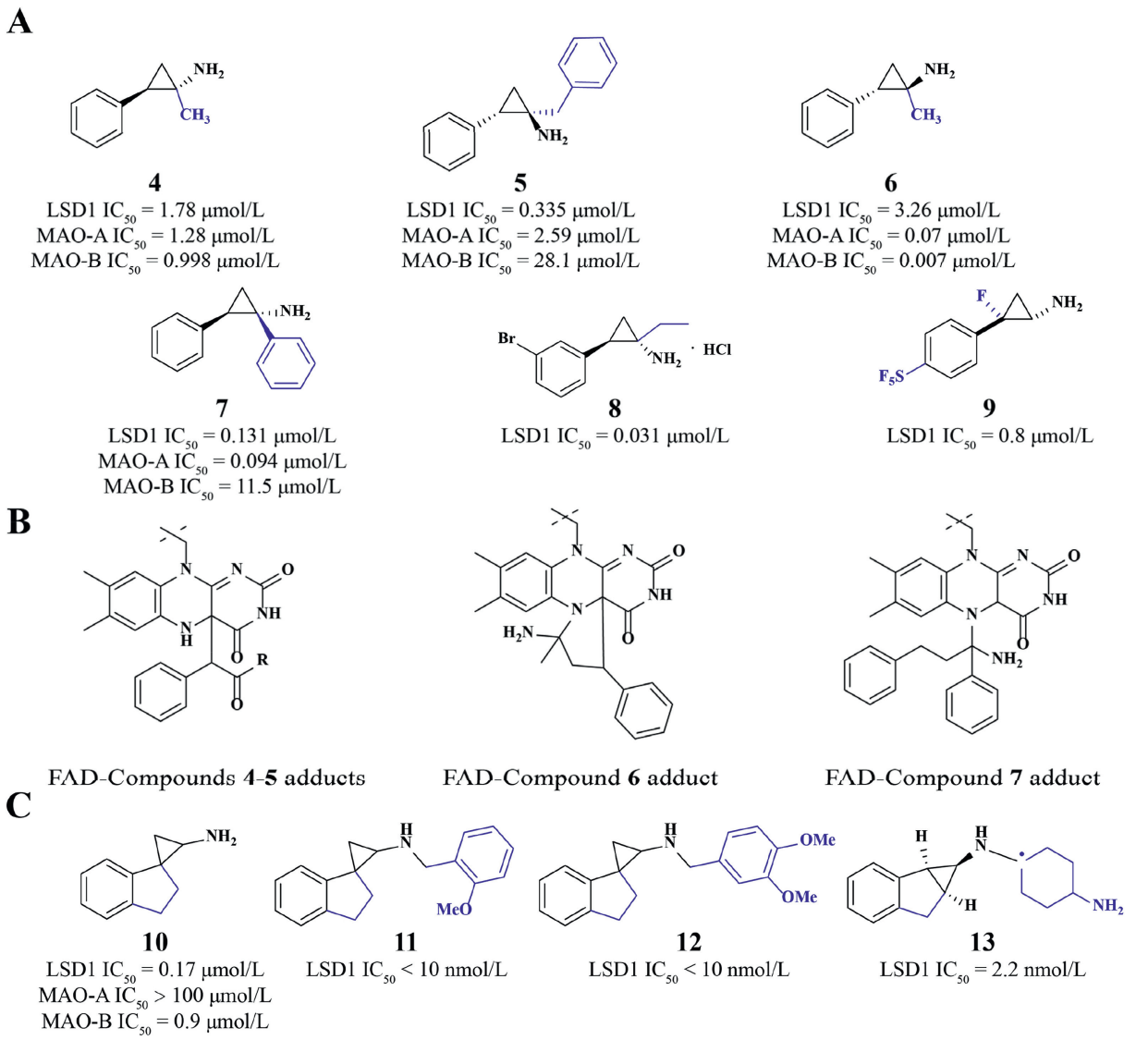

Figure 7 Chemical structures and adducts of cyclopropane core-substituted TCPs. (A) Chemical structures of α- or β-modified TCPs. (B) The adduct types of α- or β-modified TCPs. (C) Chemical structures of conformationally constrained TCP-based LSD1 inhibitors.

2.1.2. MAOs

MAOs consist of two distinct members, MAO-A and MAO-B, which share a conserved catalytic mechanism. These enzymes are implicated in a large number of neurological disorders, making them promising drug targets for Parkinson's disease and depression[23,24]. Although these two enzymes share a remarkable 70% sequence identity and exhibit structural similarities, they diverge in terms of the hydrophobic active sites opposite the flavin cofactor. Different from the monopartite cavity of MAO-A (~550 Å^3), MAO-B features a bipartite cavity composed of a substrate cavity (pocket 1, ~290 Å^3) and an entrance cavity (pocket 2, ~400 Å^3) (Fig. 8)[49,50]. The different isoforms of MAOs exhibit distinct roles in neurotransmitter metabolism and behavior, which has sparked renewed interest in the therapeutic potential of MAO inhibitors[23]. MAO-A inhibitors have shown therapeutic value against depression and anxiety disorders, while MAO-B inhibitors are commonly used to treat a variety of neurodegenerative diseases, such as Alzheimer's and Parkinson's[51]. These findings emphasize the need to develop highly specific MAOs inhibitors.

TCP was the first-generation irreversible and nonselective MAOs inhibitor (MAO-A K_i = 102 μmol/L; MAO-B K_i = 16 μmol/L)[12]. The distinct difference in the size of the MAO-B cavity compared to that of MAO-A may elucidate TCP's diverse affinities and specificities[49]. It as important to note that different enantiomers of TCP show varying selectivity for MAO isoforms. The (+)-*trans*-TCP had moderate selectivity for MAO-A, while the less active (−)-*trans*-TCP is selective for MAO-B[51]. The difference in active-site residues in the AOs family caused the formation of distinct FAD-TCP covalent adducts[20]. Crystallographic analysis of MAO-B in complex with TCP (PDB code: 2XFU) showed that both enantiomers adopted the same orientation and identical C_{4a} binding modes, differing from the major five-membered ring of the FAD-TCP adduct formed during LSD1 inactivation (Fig. 9)[52]. The phenyl ring of TCP was positioned within a hydrophobic lateral cavity of the substrate binding pocket

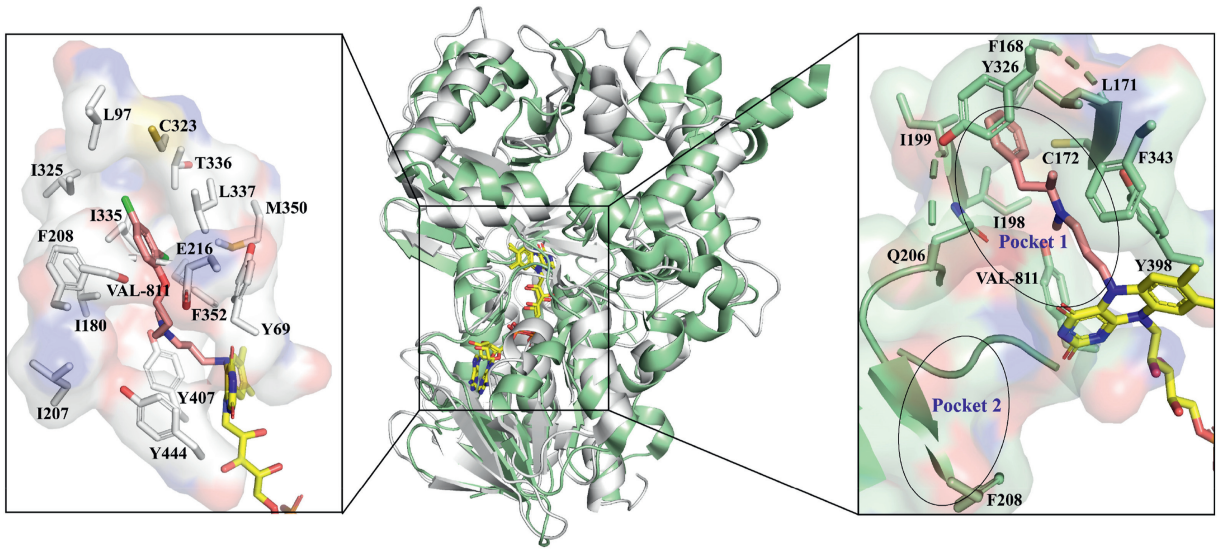

Figure 8 Structural features of MAO-A (white cartoon, PDB code: 2BXR) and MAO-B (palegreen cartoon, PDB code: 2BYB). FAD: yellow sticks.

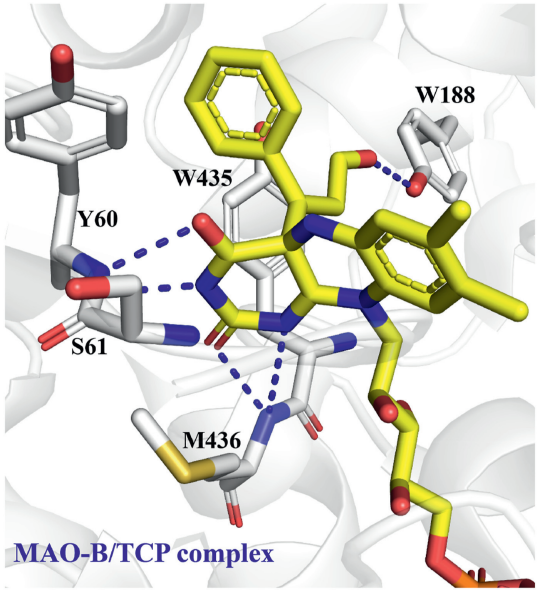

Figure 9 The binding mode of TCP in complex with MAO-B (PDB code: 2XFU). FAD-TCP adduct: yellow sticks. Hydrogen bond: blue dotted lines.

away from the flavin ring, similar to that in LSD1/(+)-*trans*-TCP complex. Several hydrogen bond interactions were observed between the adduct and residues Tyr60, Ser61, Trp188, and Met436 in MAO-B[52]. Through suppressing the activity of MAO-A and B irreversibly, TCP treatment impeded the catabolism of serotonin and norepinephrine, leading to an elevation in $GABA_B$ level within brain[3,4]. However, despite its approval as an antidepressant drug, TCP was not commonly used today due to dietary restrictions and the prevalence of common side effects.

1-Phenylcyclopropylamine (1-PCPA) was an MAO-B inactivator by forming covalent adducts with MAO-B through two distinct mechanisms. In MAO-B, a similar single-electron transfer mechanism from 1-PCPA to the flavin have been proposed (Fig. 10)[53]. The hemolytic cleavage of the cyclopropyl ring in 1-PCPA results in the formation of a carbon radical intermediate, along with the generation of flavin semiquinone and an amine radical cation. In pathway A, the adduct is formed through binding to the cysteine residue in MAO-B reversibly. The hydrogen atom transferred from a cysteine residue to the flavinsemiquinone provides the cysteine radical, which then reacts with the carbon radical intermediate to yield the cysteine adduct. Finally, the cysteine adduct is decomposed to acrylophenone. In pathway B, the covalent adduct is formed irreversibly by conjugating 1-PCPA to flavinsemiquinone. Three types adducts with covalent linkage between 1-PCPA and C_{4a}, N_5 or C_6 atoms of the reduced flavin moiety are identified[53]. Among them, the C_{4a} adduct is more flexible than the N_5 adduct, as the C_{4a}-position of flavin factor serves as a better leaving group. The C_{4a} adduct can be decomposed to acrylophenone more rapidly, resulting in the N_5 adduct. Besides, another possibility is also proposed. Firstly, the adduct adopts N_5 configuration. Then it shifts to the C_{4a} position on the isoalloxazine ring due to the reaction of lumiflavin-benzyl adduct. Considering the structural similarity of MAOs, it is possible that the MAO family shares the same inactivation mechanism[53].

The potency of *cis* and *trans* isomers of TCP against MAO-A and MAO-B does not differ significantly, whereas the substitution types and positions on the cyclopropyl ring or the phenyl ring, as well as the absolute configuration of TCP analogs, affected the potency and selectivity[53]. The SARs studies showed that introducing fluorine attachments in the β-position of the cyclopropane ring and/or substituents in the *para* position of phenyl ring favored the inhibitory potency and selectivity of TCP analogs (Fig. 11). *trans*-**14** with a methyl substituent at the α-position of the cyclopropyl ring showed comparable potency against MAOs as TCP (MAO-A IC_{50} = 0.062 μmol/L; MAO-B IC_{50} = 0.063 μmol/L), whereas *cis*-**14** (MAO-A IC_{50} = 2.3 μmol/L; MAO-B IC_{50} = 0.47 μmol/L) displayed 10-fold less potency than TCP. Moreover, compound **15** (*trans* isomer: MAO-A IC_{50} = 72 μmol/L; MAO-B IC_{50} = 20 μmol/L; *cis* isomer: MAO-A IC_{50} = 720 μmol/L; MAO-B IC_{50} = 33 μmol/L) with a β-methyl substituent on the cyclopropyl ring was much less potent against MAO-A and

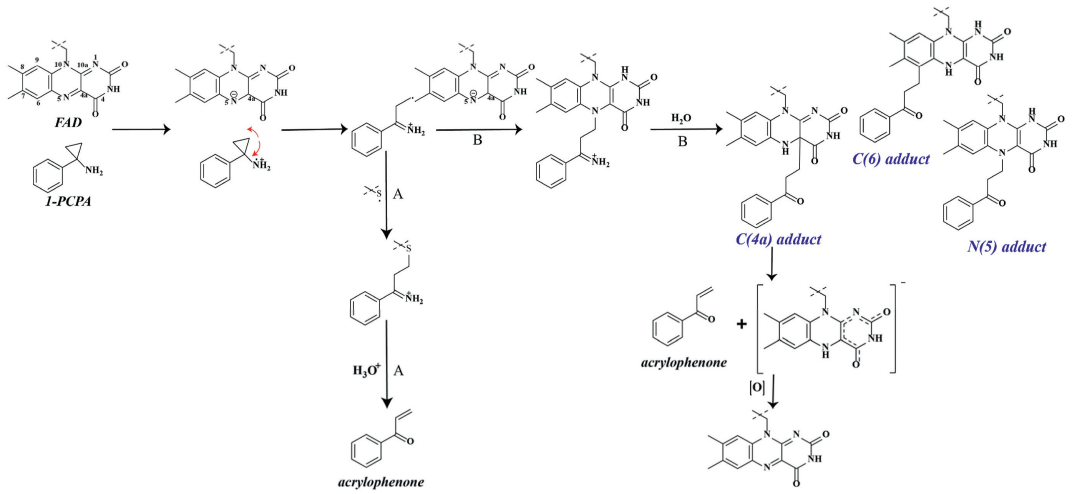

Figure 10 Proposed inhibitory mechanism of 1-PCPA against MAOs.

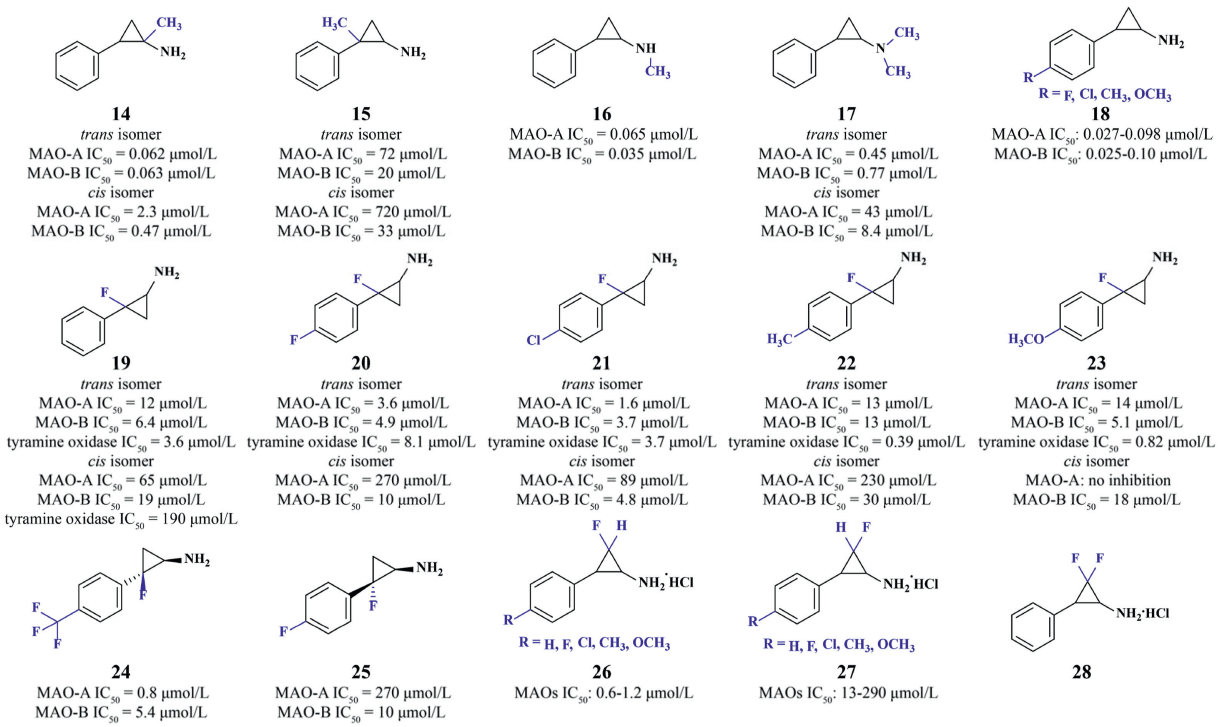

Figure 11 Chemical structures of TCPs as MAOs inhibitors.

MAO-B than TCP and **14**. Introducing the methyl group to the amine group of TCP (**16**: MAO-A IC_{50} = 0.065 μmol/L; MAO-B IC_{50} = 0.035 μmol/L) also enhanced the potency. In contrast, *N*,*N*-dimethyl substitutions in compound **17** (*trans* isomer: MAO-A IC_{50} = 0.45 μmol/L; MAO-B IC_{50} = 0.77 μmol/L; *cis* isomer: MAO-A IC_{50} = 43 μmol/L; MAO-B IC_{50} = 8.4 μmol/L) were not favorable for the potency against MAO-A and MAO-B, especially for the *cis*-isomer. This observation further confirmed that dialkylation of the amine group in TCP could decrease the potency against amine oxidases, including MAOs.

Substitution with various groups (−F, −Cl, $-CH_3$, or $-OCH_3$) at the *para*-position of the phenyl ring (**18**: MAO-A IC_{50} range: 0.027−0.098 μmol/L; MAO-B IC_{50} range: 0.025−0.10 μmol/L) also enhanced the potency against MAOs[53]. Additionally, fluorinated TCPs displayed selective inhibition against different MAO isoforms (Fig. 11)[54]. *Trans*-compounds displayed moderate selectivity against MAO-A, while *cis*-counterparts were MAO-B selective. Compared to TCP, the *trans*-isomer **19** (*trans*: MAO-A IC_{50} = 12 μmol/L; MAO-B IC_{50} = 6.4 μmol/L; *cis*: MAO-A IC_{50} = 65 μmol/L; MAO-B IC_{50} = 19 μmol/L) displayed much higher potency against MAOs, while the corresponding *cis*-isomer showed significantly lower inhibition against MAO-A and comparable potency against MAO-B[55]. Furthermore, introducing electron-withdrawing (−F and −Cl) and/or electron-donating groups ($-CH_3$ and $-OCH_3$) at the *para*-position also affected the potency against MAOs[56]. Compounds **20** (*trans* isomer: MAO-A IC_{50} = 3.6 μmol/L; MAO-B IC_{50} = 4.9 μmol/L; *cis* isomer: MAO-A IC_{50} = 270 μmol/L; MAO-B IC_{50} = 10 μmol/L) and **21**

(*trans* isomer: MAO-A IC_{50} = 1.6 μmol/L; MAO-B IC_{50} = 3.7 μmol/L; *cis* isomer: MAO-A IC_{50} = 89 μmol/L; MAO-B IC_{50} = 4.8 μmol/L) showed increased inhibitory potency against MAOs relative to *trans*-**19**, while compounds **22** (*trans* isomer: MAO-A IC_{50} = 13 μmol/L; MAO-B IC_{50} = 13 μmol/L; *cis* isomer: MAO-A IC_{50} = 230 μmol/L; MAO-B IC_{50} = 30 μmol/L) and **23** (*trans* isomer: MAO-A IC_{50} = 14 μmol/L; MAO-B IC_{50} = 5.1 μmol/L; *cis* isomer: MAO-A: no inhibition; MAO-B IC_{50} = 18 μmol/L) displayed slight reduced potency. For the corresponding *cis*-series, substituting the *para* position of the aromatic ring significantly led to decreased inhibitory activity against MAO-A with IC_{50} > 89 μmol/L. The *trans*-**24** (MAO-A IC_{50} = 0.8 μmol/L; MAO-B IC_{50} = 5.4 μmol/L) displayed about 7-fold selectivity against MAO-A over MAO-B. The *cis*-**25** (MAO-A IC_{50} = 270 μmol/L; MAO-B IC_{50} = 10 μmol/L) showed 27-fold selectivity against MAO-B over MAO-A[54].

Compounds **26** and **27**, bearing both electron-donating groups (−CH_3, −OCH_3) and electron-withdrawing groups (−Cl, −F) at the *para*-position of the phenyl ring, showed modestly enhanced potency against MAOs with IC_{50} ranges of 0.6−1.2 and 13−290 μmol/L, respectively[56]. However, compound **28** with geminal difluor substituent exhibited a 100-fold potency decrease compared to the monofluorinated analog, indicating that one fluorine substituent on the cyclopropyl ring of TCP was favored for the enhanced potency towards MAOs (Fig. 11)[56].

Collectively, the active site of MAO-A, compared to MAO-B, contains a much deeper hydrophobic cavity that can accommodate the phenyl group and cyclopropyl backbone of compounds and mediates additional interactions between the substitutions near the *para* position of the bound inhibitor and surrounding residues in MAO-A. These additional interactions may contribute to the higher potency of compounds against MAO-A over MAO-B due to the much deeper hydrophobic active site of MAO-A. Additionally, the stereochemistry of the compounds also impacts on the potency[53]. However, whether the substituent groups around the TCP scaffold affect the formation and/or features of covalent adducts with FAD is an open question to be answered, fully understanding the underlying adduct formation mechanisms may benefit the design of potent and selective MAOs inhibitors.

2.2. *Copper amine oxidases*

CuAOs that contain Cu^{2+} and a tyrosine-derived quinone cofactor are classified into two non-homologous families: the lysine tyrosylquinone (LTQ)-dependent lysyl oxidase (LOX) family and 2,4,5-trihydroxyphenylalanine quinone (TPQ)-dependent CuAOs[57]. CuAOs are involved in the metabolism of biogenic primary amines *via* catalyzing the conversion of primary amines to aldehydes and the generation of hydrogen peroxide and ammonia[57]. The mammalian LOX can initiate cross-linkage in elastin and collagen by catalyzing the oxidation of peptidyl lysine to peptidyl α-aminoadipic-δ-semialdehyde[58].

TCP was identified as a both inhibitor and substrate of lysine oxidase. *Via* inhibiting the oxidation of alkylamine (IC_{50} = 386 μmol/L) and elastin (IC_{50} = 375 μmol/L) substrates, TCP suppressed the insolubilization of collagen and elastin fibers in the wound healing and development process[53]. Additionally, cyclopropylamine, which does not contain the phenyl ring of TCP, also competitively inhibited lysyl oxidase (K_i = 516 μmol/L) while not acting as a substrate[59]. Due to the benzene ring, the cyclopropylamine ring in TCP adopted a different orientation in the active site of lysyl oxidase from that of cyclopropylamine. The cyclopropyl ring of cyclopropylamine occupied critical sites that provide interactions for the phenyl ring of TCP with lysyl oxidase[53]. A possible oxidation mechanism of TCP by LOX is shown in Fig. 12[53]. First, a Schiff base adduct (A) with the carbonyl group of the *O*-carbonyl cofactor is formed, along with the opening of the cyclopropyl ring to produce the α,β-unsaturated intermediate (B). Subsequently, the α,β-unsaturated intermediate is hydrolyzed with the production of the reduced enaminohydroxyl form of the cofactor (C) and cinnamaldehyde. Then the aminophenol is oxidized by oxygen and D is hydrolyzed to form active enzyme E and ammonia[59].

Fluorinated phenylcyclopropylamine derivatives also displayed inhibitory activity against microbial tyramine oxidase from *Arthrobacter* sp (Fig. 11)[60-62]. The SARs showed either the isomer type, relative position of amine and fluorine, *para* substituents on the phenyl ring, or the absolute configuration of compounds influenced the potency and/or selectivity of fluorinated phenylcyclopropylamines[60-62]. Among them, the *trans*-**19** (tyramine oxidase IC_{50} = 3.6 μmol/L) with a *cis* arrangement of amino and fluorine group against tyramine oxidase exhibited 10-fold higher

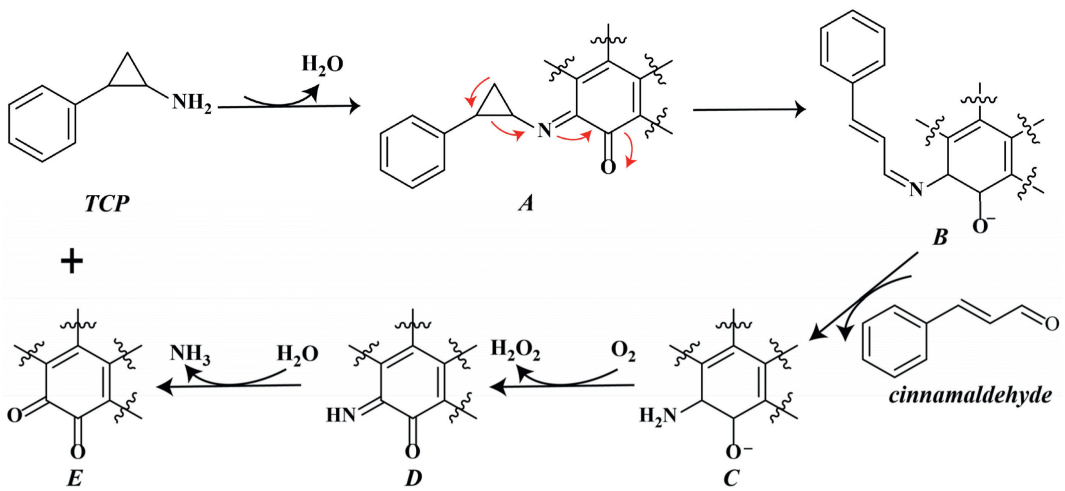

Figure 12 Proposed oxidation mechanism of TCP by lysyl oxidase.

inhibitory potency and selectivity than the non-fluorinated TCP (tyramine oxidase IC_{50} = 33 μmol/L). In contrast, *cis*-**19** (tyramine oxidase IC_{50} = 190 μmol/L), with a *trans* configuration of the fluoro and amine groups, was less potent and exhibited poor selectivity. This may be explained by the favored five-membered chelation caused by the chelation of copper with the fluorine and amino groups of the *cis* isomer. The configuration of compounds also influenced their potency. (1*S*, 2*S*)-**19** showed greater potency than racemic **19**, whereas (1*R*, 2*R*)-**19** exhibited the opposite effect[60]. Besides, substitutions on the *para* position of 2-fluoro-2-arylcyclopropylamines also improved potency against tyramine oxidase, though they did not enhance selectivity[61]. In the series of *cis* arrangement of the fluoro and amino groups, the *trans* isomers **20** (tyramine oxidase IC_{50} = 8.1 μmol/L) and **21** (tyramine oxidase IC_{50} = 3.7 μmol/L) with *para*-substituted electron-withdrawing groups (F, Cl) displayed slightly decreased inhibitory activity against tyramine oxidase compared to *trans*-**19**, whereas the potency of *trans* isomers **22** (tyramine oxidase IC_{50} = 0.39 μmol/L) and **23** (tyramine oxidase IC_{50} = 0.82 μmol/L) with electron-releasing groups (CH_3, OCH_3) was increased by ~ 10-fold[61].

TCP was also identified as an inhibitor of CuAOs isolated from *Escherichia coli* amine oxidase (ECAO), bovine plasma amine oxidase (BPAO), equine plasma amine oxidase (EPAO), *Arthrobacter globiformis* amine oxidase (AGAO) and semicarbazide-sensitive amine oxidase (SSAO)[4,63]. However, there is limited information on TCP analogs targeting these CuAOs. The structure of ECAO complexed with TCP (PDB code: 1LVN) showed that TCP was located in the active sites of the homodimeric ECAO by forming an adduct analog to the phenylethylamine substrate Schiff's base intermediate, with ring position 5 of the quinone cofactor TPQ (Fig. 13A). The phenyl ring of the (+)-TCP that bound in the hydrophobic concave roof of narrow substrate entry/exit channel made *van der Waals* contacts with Phe192, Thr223-Leu225 and Val463-Gly464. Moreover, *van der Waals* contacts were also observed between the cyclopropyl ring of (+)-TCP and residues Val463 and catalytic Asp383 (Fig. 13B)[64].

SSAO is a CuAOs enzyme involved in the primary metabolization pathway of histamine, and SSAO alterations are also associated with different psychiatric disorders. However, unlike its inhibition against FAOs, TCP treatment led to the increased activity of SSAO[4,63]. This is probably due to the intrinsic enzyme induction in the SSAO itself and/or from changing levels of an endogenous modulator[65]. The inhibition of SSAO may be one of the reasons for TCP's side-effect as an antidepressant to inhibit the FAOs in the brain[64].

3. Cytochrome P450s superfamily

The CYP superfamily can oxidize, peroxide, and reduce endogenous and xenobiotic substrates such as prostaglandins, steroids and fatty acids, playing central roles in steroid synthesis, fatty acid metabolism, and chemical defense[66,67]. The catalytic activities of CYPs are important considerations in endocrine function and drug−drug interactions[68]. By targeting the CYP superfamily, TCP may serve as a privileged scaffold in drug discovery for treating human diseases[3,69].

CYP46A1 (cholesterol 24-hydroxylase) is a rate-limiting enzyme for cholesterol degradation, which has neuroprotective effect in Huntington's disease and Alzheimer's disease. Restoring CYP46A1 activity in the striatum opens new avenues for treating neurodegenerative diseases[70]. In addition, dysregulation of CYP46A1 impairs the morphology and function of mitochondrial, leading to the accumulation of lipid droplet (LD). Abnormal LD metabolism is implicated in a variety of disorders, particularly nonalcoholic fatty liver disease (NAFLD)[71]. TCP can completely inhibit cholesterol 24-hydroxylation by binding to CYP46A1 with low nanomolar affinity[69]. Crystal analysis of CYP46A1/TCP complex (PDB code: 3MDR) showed that TCP interacted with the heme iron in CYP46A1 with an N−Fe distance of 2.23 Å (Fig. 14). The benzene ring of TCP was located between the side chains of Phe121 and Thr475, forming *van der Waals* contacts with Ile301, Ala302, and Thr306. The amine of TCP formed direct or water-mediated hydrogen bonds with the surrounding residues Ala302, Thr306 and Ser307. TCP binding induced a conformational change in residues Leu112 and Phe121 in the CYP46A1 active sites, leading to volume and shape alternations in the active site and blocking substrate access[69]. CYP8A1 is a

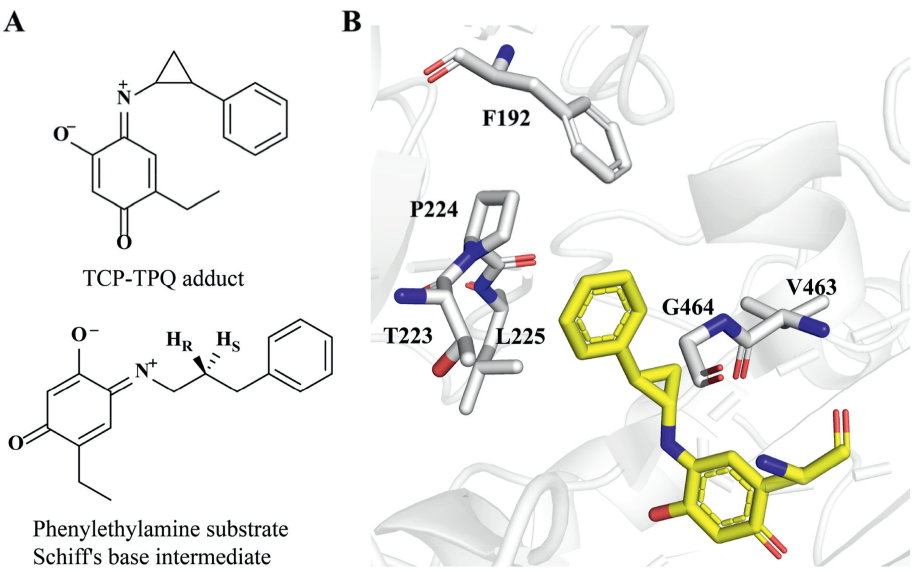

Figure 13 (A) The binding model of ECAO in complex with TCP (PDB code: 1LVN). Yellow sticks: TCP-TPQ adduct. (B) The adduct types formed in the ECAO complexes.

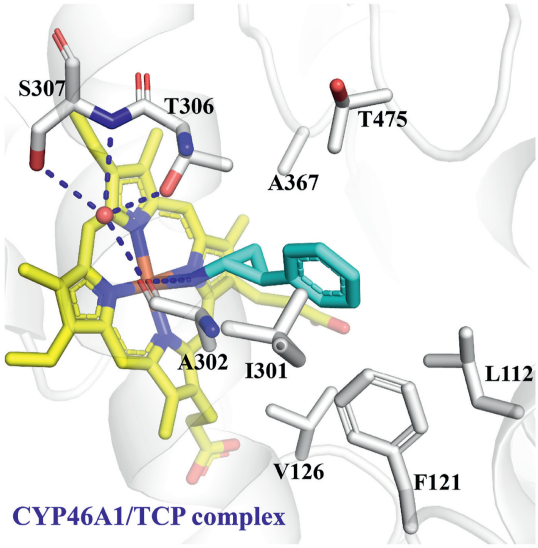

Figure 14 The binding mode of CYP46A1 in complex with TCP. CYP46A1: white cartoon. Heme iron: yellow sticks. TCP: cyan sticks. Hydrogen bond: blue dotted lines.

prostacyclin synthase that plays role in the biosynthesis of prostacyclin (PGI2). It can inhibit platelet activation and displays anti-inflammatory effect[72]. By targeting CYP8A1, TCP also showed anti-inflammatory activity and played roles in regulating PGI2-mediated cardiovascular and hemostasis functions[3].

Additionally, the CYPs superfamily is crucial in pharmacokinetic drug interactions and inter-individual variability in drug metabolism[73]. Genetic polymorphisms of CYP genes can result in differences in drug response and altered risk for adverse drug reactions[73]. Among the CYPs enzymes, CYP2A6 is primarily expressed in hepatic cells and is one of the most important enzymes mediating nicotine metabolism. Biochemical assay showed that TCP was a potent and selective inhibitor of CYP2A6 with a K_i value of 0.08 μmol/L[3]. Nevertheless, CYP2A6 inhibition by TCP was of low clinical significance due to the minor contribution of CYP2A6 in drug metabolism[3]. Moreover, TCP also displayed inhibitory activity against other members of the CYPs family, including CYP2C9 (K_i = 56 μmol/L), CYP2C19 (K_i = 32 μmol/L) and CYP2D6 (K_i = 367 μmol/L). Although none of these inhibitory effects are clinically significant at therapeutic doses of TCP, it is crucial to be aware of the possible pharmacokinetic drug interaction issues of TCP derivatives[3].

It was observed that the inhibition potency and selectivity of TCP towards CYPs were highly dependent on its amine group (Fig. 14). Cyclopropylbenzene, which lacked the amine group of TCP, showed significantly less potency against CYP1A, CYP2A6, CYP2C19, and CYP2E1 and no activity towards CYP2D6, CYP2C9 and CYP3A4. This indicated that the amine group of TCP was essential for its inhibitory activity and selectivity towards CYPs. The reduced amphiphilicity and intrinsic lipophilicity caused by the amine group may be responsible for the higher potency of TCP against selected CYPs[53].

4. Cellular receptors

TCP derivatives also bind to various cellular receptors, such as 5-HT receptor, platelet $P2Y_{12}$ receptor, epidermal growth factor receptor (EGFR), Dopamine D3 receptor, and Smoothened receptor.

4.1. 5-HT receptor

The central serotonin 5-HT receptors, consisting of three members (5-HT_{2A}, 5-HT_{2B}, and 5-HT_{2C}), are widely distributed throughout the central nervous system (CNS) and mediate various biological processes such as mood, appetite, and sexual behavior. 5-HT receptors are involved in obesity, cognition, addiction, and neurological disorders, highlighting their value as potential drug targets for CNS-related disorders. The 5-HT receptor agonists are typically characterized by a common scaffold that connects an aromatic ring to ionizable nitrogen *via* a 2−3 atoms (C and or N, usually C) linker[74].

N,*N*-Dialkylated TCP derivatives were identified as active 5-HT receptor agonists (Fig. 15). The SARs studies showed that the enantiomeric form, the substitution pattern of the phenyl ring, or the alkyl groups on the amino group influenced the 5-HT receptor stimulating activity of TCP analogs[75]. Among them, **24** and **25** were the most potent 5-HT receptor agonists. Only the (1*R*, 2*S*)-enantiomers (−)-**24** and (−)-**25** displayed activity towards rat brain 5-HT receptor with 5-HT formation ED_{50} range of 0.26−0.38 μmol/(L*kg), whereas the (1*S*, 2*R*)-enantiomers (+)-**24** and (+)-**25** were inactive (5-HT formation $ED_{50} > 50$ μmol/(L*kg). Replacing the *N*,*N*-di-*n*-propyl groups in **24** and **25** with *N*,*N*-dimethyl or *N*,*N*-di-*n*-butyl groups significantly decreased their potency compared to their counterparts. Moreover, replacing the hydroxyl groups on the phenyl ring in **24** and **25** with the methoxy motif also reduced the activity towards rat brain 5-HT receptor with 3−4 folds[75]. The *N*,*N*-di-*n*-propyl substituted derivatives (**26**−**30**) were designed by retaining the *N*,*N*-dipropylcyclopropylamine moiety and modifying the aromatic ring (Fig. 15). The SARs studies showed that introducing electron-rich aryl groups enhanced affinity for the 5-HT_{1A} receptor, whereas electron-withdrawing substituents had the opposite effect[76]. The 2-hydroxy-5-fluorophenyl derivative **27** showed decreased affinity towards 5-HT_{1A} receptor with K_i value of 99 nmol/L than the phenyl derivative **26** (5-HT receptor K_i = 24 nmol/L). The (1*R*, 2*S*)-isomer of **27** (5-HT receptor K_i = 3.2 nmol/L) was an effective 5-HT_{1A} receptor agonist with 8-fold higher potency than its counterpart (1*S*, 2*R*)-isomer (5-HT receptor K_i = 348 nmol/L). Compound **28** (5-HT receptor K_i = 13 nmol/L) and **29** (5-HT receptor K_i = 21 nmol/L) with the 2- and 3- thienyl ring, respectively, had enhanced potency than **26**. However, **30** with 2-benzothienyl ring was an ineffective 5-HT_{1A} receptor agonist with K_i value > 1000 nmol/L due to the additional bulk caused by the aromatic moiety[76].

The modified *trans*-2-(indol-3-yl)cyclopropylamine derivatives with 4-OCH_3 (**32**), 5-OCH_3 (**33**), or 5-F groups (**34**) displayed enhanced affinity towards 5-HT receptor than the unsubstituted compound **31** (Fig. 15)[77]. Compound **33** (5-HT_{2A} receptor K_i = 40 nmol/L) with the 5-methoxy substitution displayed the highest potency against the 5-HT_{2A} receptor, while compound **34** with a 5-fluoro substitution (5-HT_{2A} receptor K_i = 1.9 nmol/L) was the most efficacious 5-HT_{2C} agonist. The (1*R*, 2*S*)-isomer of **35** showed much higher affinity towards 5-HT_{2A} and 5-HT_{2B} receptors, while the (1*S*, 2*R*)-isomer of **36** was efficacious towards 5-HT_{2C} receptor. This reversal of stereoselectivity favored the development of selective 5-HT_{2C} receptor agonists[77]. Introducing cyclopropane motif may increase affinities of compounds towards the 5-HT_2 receptor family than the phenethylamine derivatives[78]. Compound **37**, a cyclopropane analog of hallucinogenic

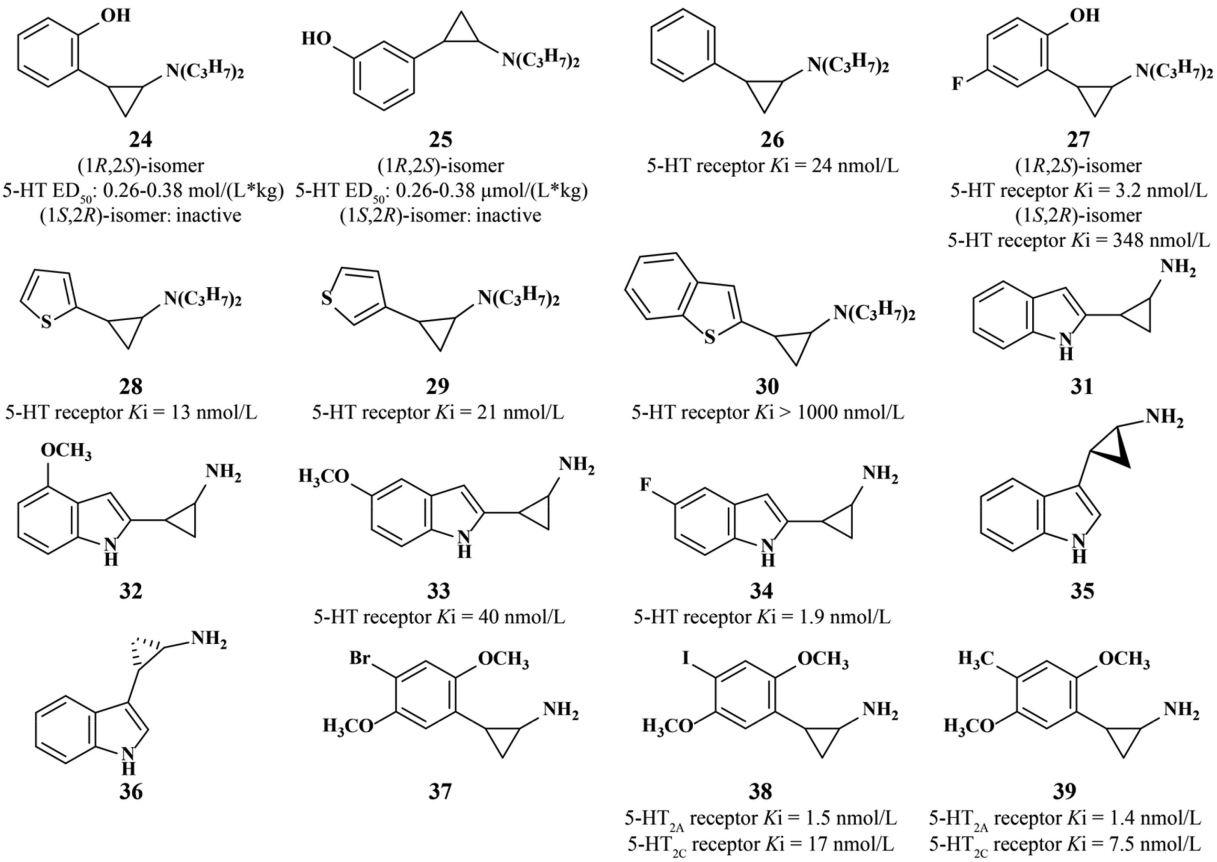

Figure 15 Chemical structures of TCP-based 5-HT receptor agonists.

amphetamine, was identified as a highly potent 5-HT_{2A} agonist both *in vivo* and *in vitro*[79]. Halogen-substituted cyclopropane analogs **38** (5-HT_{2A} receptor K_i = 1.5 nmol/L; 5-HT_{2C} receptor K_i = 17 nmol/L) and **39** (5-HT_{2A} receptor K_i = 1.4 nmol/L; 5-HT_{2C} receptor K_i = 7.5 nmol/L), especially the compound with (−)-(1*R*, 2*S*)-configuration, showed increased potency for the 5-HT_2 receptor family[78].

4.2. Platelet P2Y12 receptor

Platelet $P2Y_{12}$ receptor, a key player in platelet activation, is a drug target for suppressing platelet aggregation and atherothrombotic events[80,81]. 2-phenylcyclopropylamine-nucleoside conjugates were $P2Y_{12}$ receptor antagonists. The TCP moiety, especially the (1*R*, 2*S*)-isomer, was vital for achieving high potency and good pharmacokinetics properties of $P2Y_{12}$ antagonists[82]. The cyclopentyl triazolopyrimidine, an isosteric analog of adenosine, can allosterically bind to the $P2Y_{12}$ receptor to lock it in the inactive conformation state. Subsequently, the ADP signaling was suppressed[83]. Ticagrelor (h$P2Y_{12}$ pK_i = 8.7) was the first oral reversible $P2Y_{12}$ receptor antagonist approved to reduce the risk of myocardial infarction, cardiovascular death and stroke in patients with ACS. By inhibiting $P2Y_{12}$ receptor-induced vasoconstriction and inflammation, ticagrelor can prevent vasospasm and restenosis[6]. However, ticagrelor also acted as an inhibitor against CYP3A4, which contributed to drug−drug interactions. Thereby, pharmacokinetic drug interaction was an issue when co-administered with compounds targeting CYP3A. Compound **40** (h$P2Y_{12}$ pK_i = 8.3) showed acceptable affinity and metabolic stability. Additionally, tetrazole-containing derivative

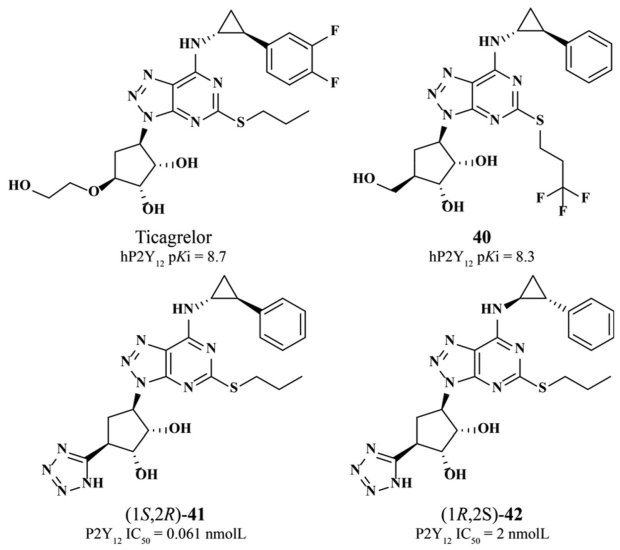

Figure 16 Chemical structures of 2-phenylcyclopropylamine-nucleoside conjugates targeting platelet $P2Y_{12}$ receptor.

41 and **42** were highly potent $P2Y_{12}$ antagonists by inhibiting ADP-induced washed platelet aggregation. However, relative to the (1*R*, 2*S*)-**42** ($P2Y_{12}$ receptor IC_{50} = 2 nmol/L), (1*S*, 2*R*)-**41** ($P2Y_{12}$ receptor IC_{50} = 0.061 nmol/L) showed 30-fold increase (Fig. 16)[84]. Residue Lys280 in $P2Y_{12}$ receptor was a critical residue for interacting with other $P2Y_{12}$ antagonists (*e.g.*, GTDC and AZD1283). Docking analysis showed that the benzene ring of

TCP scaffold in ticagrelor mediated the π−H interaction with Lys280 of the $P2Y_{12}$ receptor, highlighting the vital role of the TCP scaffold in $P2Y_{12}$ inhibition[85].

4.3. EGFR

EGFR, a receptor tyrosine kinase, plays critical roles in initiating signal transduction pathways in epithelial cells. As a major oncogenic driver, overexpression of EGFR is closely associated with cellular proliferation, survival, and metastasis in various cancers[86]. In addition to conventional EGFR inhibitors and monoclonal antibodies[86], installation of the TCP fragment into the quinoline ring afforded new EGFR inhibitors[87,88]. Compound **43** potently inhibited EGFR (IC_{50} = 0.01 μmol/L) and suppressed cell proliferation of KB cells (KB cells IC_{50} = 0.14 μmol/L) (Fig. 17)[87]. To further improve its pharmacokinetic property, the 4-(2-aryl-cyclopropylamino)-quinoline-3-carbonitrile derivatives were prepared[88]. The SARs results showed that the alkoxy substituents at both C-6 and C-7 positions favored the activity. Among them, compounds **44** and **45** displayed potent phosphorylation inhibition both *in vitro* and *in vivo*, with IC_{50} ranging from 3 to 8.4 nmol/L (Fig. 17)[88].

4.4. Dopamine D_3 receptor

Dopamine D_3 receptor is involved in the regulation of dopamine release, dopaminergic function, and neurotransmitters level, making it an attractive therapeutic target for neurological diseases, such as Parkinson's disease, drug addictions, depression, and schizophrenia[89]. Served as a key dopaminergic moiety, TCP displayed weak affinity and limited selectivity against D_3 receptor over D_2 receptor (D_3 receptor K_i = 12.8 μmol/L; selectivity index = 4) (Fig. 18)[8]. To improve the potency and selectivity of TCP, a series of TCP-substituted analogs were synthesized as potent and selective dopamine D_3 receptor antagonists. The most potent compound **46** inhibited human D_3 receptors with K_i values of ~2.7 nmol/L and a selectivity of >223-fold over human D2 receptor[8]. Besides, the compounds that dual-target dopamine D_3 and μ-opioid (MOR) receptor were produced by tethering the key dopaminergic moiety *trans*-phenylcyclopropyl amine to different opioid scaffolds[90]. Acting as MOR partial agonists and D_3 receptor antagonists, compounds **47** (MOR K_i = 55.2 nmol/L; D_3 receptor K_i = 382 nmol/L) and **48** (MOR K_i = 85.2 nmol/L; D_3 receptor K_i = 361 nmol/L) displayed potential analgesic effects and reduced opioid-misuse liability[90].

4.5. Smoothened receptor

Smoothened (Smo) is a seven-transmembrane G-protein-coupled receptor (GPCR) activated by hedgehog ligands. Serving as an essential signal transducer of the canonical hedgehog (Hh) signaling pathway, Smo plays vital roles in normal embryonic development and adult tissue homeostasis[91]. Smo antagonists are emerging as potential therapeutic agents for Hh-pathway dependent malignancies, such as medulloblastoma, prostate cancer and pancreatic cancer[24]. A series of bicyclic hydantoin derivatives with TCP were identified as Smo antagonists of the Hh-pathway (Fig. 19). The SARs studies showed that both the *trans*-2-phenylcyclopropyl and hydantoin ring systems were vital for the potency of Smo antagonists. Moreover, the stereochemistry of the cyclopropyl ring was also a key determinant for the binding affinity towards Smo[92,93]. The most potent compounds, dichlorophenyl urea **49** (Smo binding IC_{50} = 220 nmol/L) and 2-biphenyl analog **50** (Smo binding IC_{50} = 94 nmol/L), suppressed the growth of medulloblastoma cells[93]. Both compounds were selected as leads for further optimization to improve their pharmacokinetic properties. Finally, MK-5710 with good pharmacokinetics properties and oral bioavailability was identified as a potent Smo antagonist (Smo binding IC_{50} = 220 nmol/L; Hh-light 2 cell IC_{50} = 17 nmol/L). MK-5710 inhibited the proliferation of medulloblastoma cells and displayed antitumor efficacy in the Hh-signaling pathway-dependent mouse allograft tumor model[92].

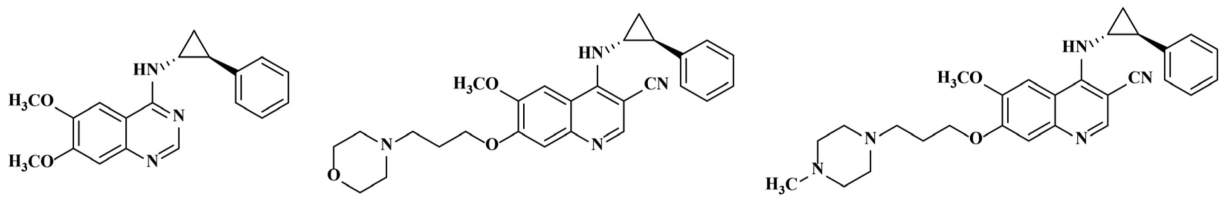

Figure 17 Chemical structures of TCP analogs targeting EGFR.

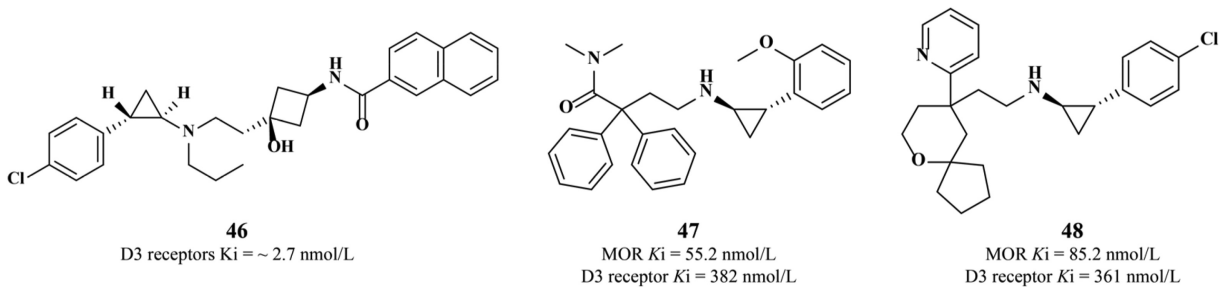

Figure 18 Chemical structures of TCP analogs targeting dopamine D3 receptor.

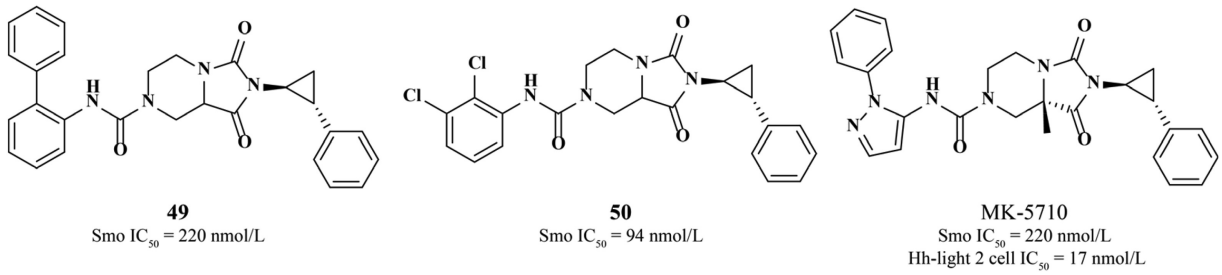

Figure 19 Chemical structures of TCP-based Smo antagonists.

4.6. Other enzymes

TCP derivatives exhibit various biological activities (*e.g.*, anti-inflammatory, prostaglandin synthesis, and hydrolysis) by inhibiting many enzymes such as soluble epoxide hydrolases (sEH), HIV-1 RT, DNA gyrase and dipeptidyl peptidase IV (DPP-IV)[6,7,9].

4.6.1. sEH

sEH is a family of ubiquitous enzymes that play a crucial role in catalyzing the hydrolysis of epoxides to more soluble and easily excretable metabolites. Through controlling the levels of biologically active epoxide mediators, sEH can regulate physiological and pathological function[94,95]. Series of 4-substituted piperidine-based trisubstituted compounds were identified as highly selective and potent sEH inhibitors. The SARs studies revealed that incorporation of a TCP scaffold led to enhanced ion channel activity. Compound **51** (sEH IC_{50} = 27 nmol/L) displayed remarkable potency and selectivity against EH, minimizing the risk of undesirable pharmacological effects on other biological targets, such as ion channels and CYPs (Fig. 20). Compound **52** (sEH IC_{50} = 565 nmol/L) was a promising hit compound for further optimization (Fig. 20)[96]. Crystallography analysis of the sEH/compound **52** complex (PDB code: 3ANS) revealed that the amine group and cyanophenyl motif of **52** formed a hydrogen bond network with residues Asp335, Tyr383, and Tyr466 within the sEH catalytic triad to stabilize the binary complex. This structural feature was consistently observed among reported the sEH inhibitors. The benzene ring of the 4-cyanophenyl group engaged in $\pi-\pi$ stacking interactions with the indole ring of Trp336, while the cyano group in **52** made *van der Waals* contacts with Met339 (Fig. 21A)[96]. With **52** as a hit compound, a series of derivatives were synthesized to further improve the absorption, distribution, metabolism, excretion, and toxicity profile through modification. Among them, the urea derivative **53**, featuring a 4-(3-*iso*-propyl-1, 2,4-oxadiazol-5-yl)piperidine, was identified as a potent sEH inhibitor with an IC_{50} value of 8.5 nmol/L against human sEH. Importantly, **53** exhibited improved aqueous solubility and reduced CYPs inhibition (Fig. 20)[96]. Structural analysis of sEH in complex with **53** (PDB code: 3ANT) showed that the 4-(3-*iso*-propyl-1, 2,4-oxadiazol-5-yl)piperidine motif in **53** fulfilled the previously unoccupied hydrophobic channel due to its increased volume, resulting in the enhanced lipophilicity. This motif also established additional *van der Waals* contact with the surrounding residues on one side of the channel, leaving the other side open (Fig. 21B)[96]. The phenyl groups in both compounds were loosely surrounded by lipophilic residues, indicating that further modification of the phenyl group may favor the potency.

The carboxylic acid-containing cyclopropyl urea derivatives **54** (human sEH IC_{50} = 4.3 nmol/L) and **55** (human sEH IC_{50} = 19.1 nmol/L) showed excellent inhibitory activity towards sEH, with minimal CYP inhibition, excellent oral absorption, and a notable reduction in renal injury, all without inducing hypotensive effects (Fig. 20)[97,98]. The X-ray structure of the sEH/**55** (PDB code: 4X6Y) showed that the 4-phenoxypiperidine and

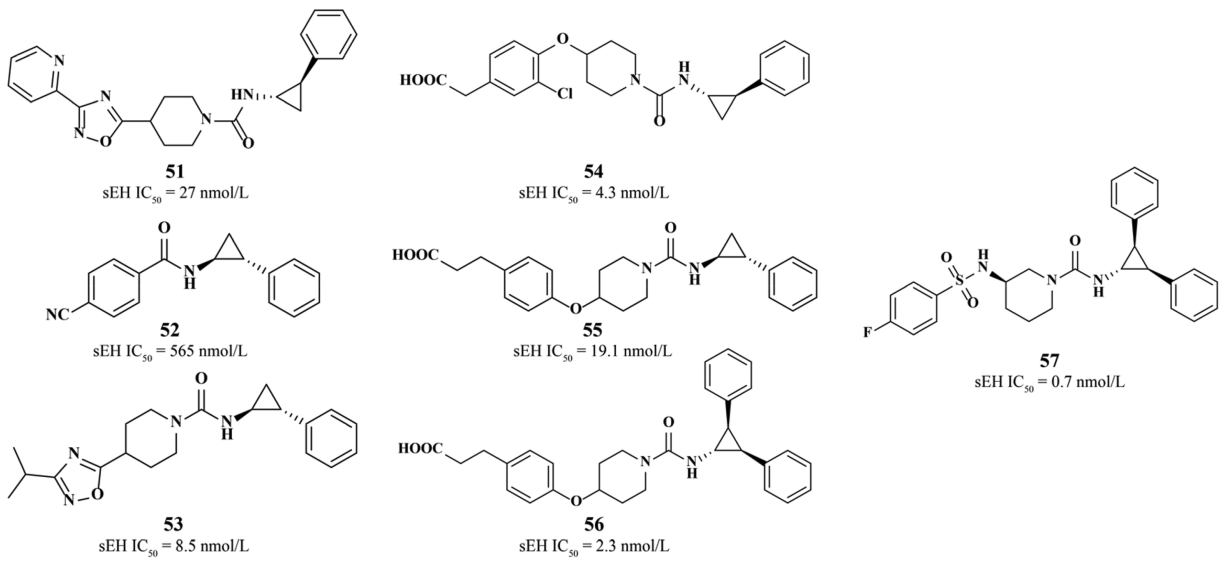

Figure 20 Chemical structures of TCP analogs targeting sEH.

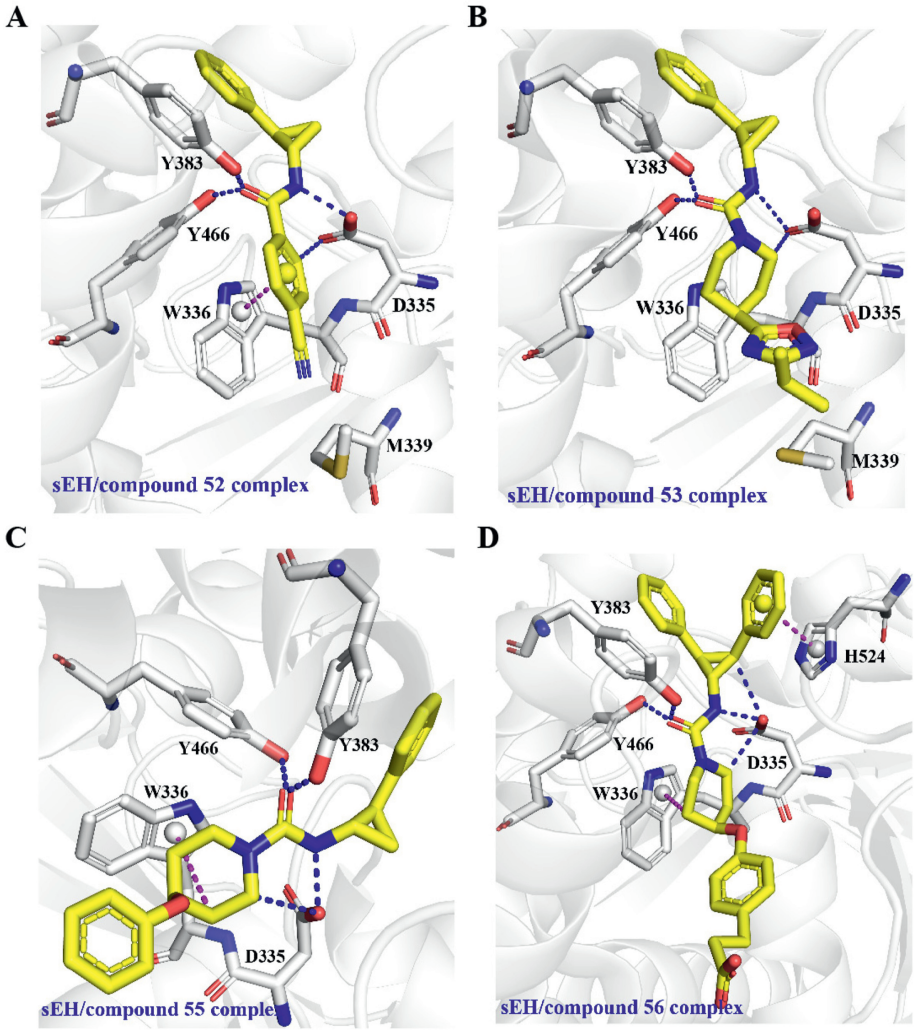

Figure 21 The binding mode of compound **52** (A, PDB code: 3ANS), **53** (B, PDB code: 3ANT), **55** (C, PDB code: 4X6Y) and **56** (D, PDB code: 4X6X) in complex with sEH. sEH: white sticks. Hydrogen bond: blue dotted lines. $\pi-\pi$ and $\pi-$H stacking interaction: magentas dotted lines.

cyclopropylphenyl motifs of **55** were located in the catalytic pocket of sEH. Notably, the region around the geminal hydrogen position of the cyclopropyl motif was unoccupied. The oxygen atoms within the carbonyl and NH groups of **89** mediated a hydrogen bond network with residues Tyr 383, Tyr 466 and the carboxylic acid of Asp 335. Additionally, the piperidine ring engaged in $\pi-$H stacking interactions with the indole ring of Trp336 (Fig. 21C)[98]. Using **55** as a lead compound, series of three substituted cyclopropane derivatives were synthesized to further enhance the potency by occupying all available pockets of sEH catalytic domain[98]. Compound **56** with a diphenyl-substituted cyclopropyl moiety exhibited good sEH inhibitory activity with an IC_{50} value of 2.3 nmol/L (Fig. 20). Co−crystal structure of sEH/**56** (PDB code: 4X6X) showed that the newly introduced phenyl group on the cyclopropyl ring mediated an additional $\pi-\pi$ interaction with residue His524 (Fig. 21D). Additionally, a 3-substituted piperidine derivative with sulfonamide **57** (human sEH IC_{50} = 0.7 nmol/L) further improved the sEH inhibitory activity (Fig. 20)[98]. In summary, the amine group and cyclopropyl ring of the TCP scaffold mediated the conversed hydrogen bond interaction that is critical for the inhibitory activity of TCP-based sEH inhibitors.

4.6.2. HIV-1 reverse transcriptase

HIV-1 RT is a heterodimeric enzyme responsible for catalyzing the reverse transcription of viral RNA genome into proviral DNA in infected cells, a crucial step in the early stage of the virus's life cycle[12,99]. Inhibitors of HIV-1 RT can be categorized into two types: nucleotide reverse transcriptase inhibitors (NRTIs) and non-nucleoside reverse transcriptase inhibitors (NNRTIs)[100]. MIV-150 and compounds **58**−**59** bearing a TCP moiety were potent NNRTIs that directly impeded the viral RT process through an allosteric mechanism (Fig. 22A)[50,101]. MIV-150, serving as a third-generation NNRTI, effectively blocked HIV-1 and HIV-2 infection with an EC_{50} of less than 1 nmol/L against HIV-1/HIV-2_{MN}[101]. Two combinational clinical trials of MIV-150 have been initiated to evaluate its safety and pharmacokinetics for HIV-1 seronegative patients (ClinicalTrials.gov Identifier: NCT02033109; NCT03408899)[12]. Crystallography analysis of HIV-1 RT/MIV-150 complex (PDB code not disclosed) showed that the urea group in MIV-150 established a hydrogen bond interaction with the backbone of residue Lys101. $\pi-$Stacking interactions were observed between the 5-cyanopyrid-2-yl motif and residues Phe227, as well as the phenyl ring and residues Tyr181 and Tyr188[100]. Additionally, the racemic cyclopropane derivatives **58** and **59** also exhibited

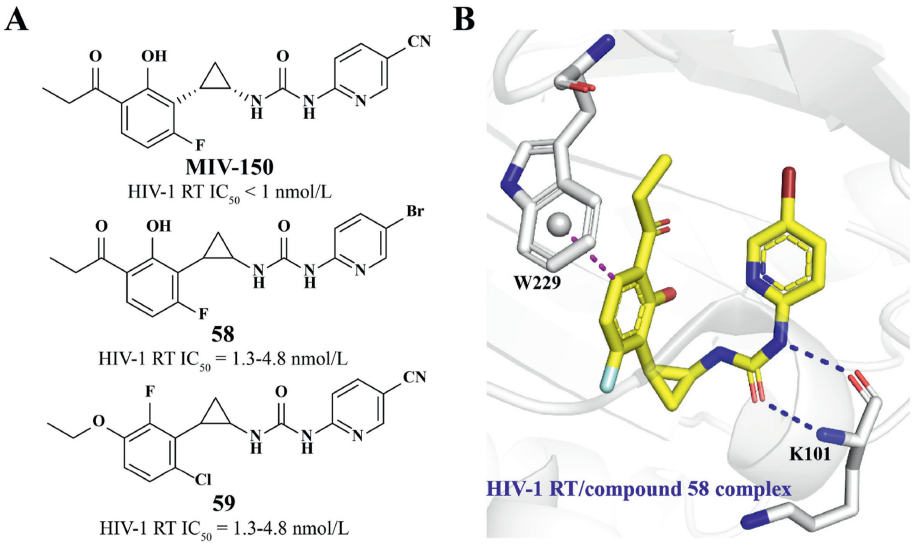

Figure 22 The TCP analogs targeting HIV-1 RT. (A). Chemical structures of TCP analogs targeting HIV-1 RT. (B) The binding mode of HIV-1 RT in complex with compound **58** (PDB code: 1EET). HIV-1 RT: white sticks. Hydrogen bond: blue dotted lines. π−H stacking interaction: magentas dotted lines.

anti-HIV-1 activity with IC_{50} range ranging from 1.3 to 4.8 nmol/L. Several conserved interactions were also observed in the HIV-1 RT/**58** complex (PDB code: 1EET), similar to that in HIV-1 RT/MIV-150 complex (Fig. 22B)[50].

4.6.3. DNA Gyrase and DPP-IV

DNA Gyrase, a member of type II topoisomerase family, can catalyze the ATP-dependent negative super-coiling of double-stranded closed-circular DNA. As a well-validated drug target for antibacterial agents, DNA Gyrase is involved in bacterial DNA replication, repair, and decatenation[102]. The ciprofloxacin-TCP conjugate **60** demonstrated potent inhibitory activity against DNA Gyrase across 12 different Gram-positive and Gram-negative microorganisms (Fig. 23). The antibacterial activity of the (1*S*, 2*R*)-enantiomer of **60** was much higher than the racemic form, (±)-**60**, and (1*R*, 2*S*)-enantiomer. This activity difference may be attributed to the selectivity of uptake[103].

DPP-IV (also known as CD26) is a prolyl dipeptidase which plays roles in the glucose-dependent insulinotropic polypeptide (GIP) and degradation of glucagon-like peptide 1 (GLP-1). By cleaving the insulin-sensing hormones at the peptide bond of the penultimate position, DPP-IV is involved in the development of chronic metabolic type 2 diabetes mellitus (T2D)[104]. However, the closely related prolyl peptidases such as DPP-II, DPP8/9, and fibroblast activation protein (FAP) can induce toxic side effects.

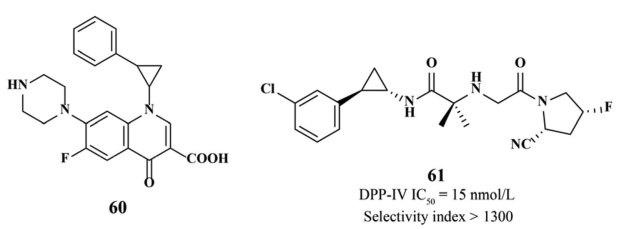

Figure 23 Chemical structures of TCP analogs targeting DNA Gyrase and DPP-IV.

This has led to the development of potent and selective DPP-IV inhibitors as antidiabetic agents[104]. A series of compounds derived from TCP were synthesized to develop long-acting DPP-IV inhibitors with improved pharmacokinetic profiles. Among them, compound **61** with favorable pharmacokinetic profiles was identified as a potent and selective DPP-IV inhibitor (DPP-IV IC_{50} = 15 nmol/L; selectivity index >1300) (Fig. 23). Moreover, *in vivo* studies demonstrated that compound **61** significantly inhibited plasma DPP-IV activity and enhanced glucose tolerance in animal models[7].

5. Conclusion and perspectives

TCP derivatives have shown various biological activities, such as antidepressant, anticancer, antiviral effects, involvement in prostaglandin synthesis and drug metabolism. This makes TCP a valuable scaffold for new drug discovery. Notably, significant progress has been made in TCP-based drug discovery. TCP itself is an antidepressant drug for the treatment of patients with major depressive disorder. Rational molecular editing on the phenyl ring, amine group, the cyclopropyl core, and the configuration of the TCP scaffold favor their potency and/or selectivity against LSD1 over other homologous enzymes, with several TCP-based LSD1 inhibitors currently undergoing clinical assessment. Ticagrelor is the first oral reversible $P2Y_{12}$ receptor antagonist approved to reduce the risk of myocardial infarction, cardiovascular death, and stroke. MIV-150, a third-generation non-nucleoside reverse transcriptase inhibitor, effectively blocks HIV-1 and HIV-2 infection. It has progressed to the clinical stage for treating HIV-1 seronegative patients suffering from acute coronary syndrome.

While the mentioned achievements have been observed, TCP-based drug discovery still encounters challenges such as pharmacokinetic issues, on/off-target toxicity, and other adverse effects. The wide target space for TCPs represents a double-edged sword—broad therapeutic promise or off-target toxicities. Due to the extensive inhibitory activity against FAD-containing enzymes or other proteins (*e.g.*, CYP450s, $P2Y_{12}$ receptor, DPP-IV and

EHs), TCP-based compounds may have broad clinical applications. The compounds binding to multiple targets could be developed, such compounds have demonstrated promising therapeutic effects. Moreover, the identified target landscape of TCPs could provide medicinal chemists with insights to investigate in-depth modes of action or potential on/off-target issues in their drug candidates containing the TCP moiety. However, TCPs may have potential unfavorable issues related to selectivity, unfavorable pharmacokinetic interactions, or off-target effects. The irreversible binding of TCP analogs to the targets could lead to on-target toxicity, including hepatotoxicity, mutagenicity, or carcinogenicity. The binding mechanism determines whether TCPs targeting different targets exhibit the same off-target toxicity. For various FAD-dependent amine oxidases, their conserved catalytic mechanism contributes to similar off-target toxicity. Furthermore, unfavorable pharmacokinetic interactions with cytochrome P450 enzymes are a common issue with TCP derivatives. The types and positions of substituents on the TCP scaffold, along with the stereochemistry of TCPs, significantly impact their inhibitory actives across diverse targets, offering valuable guidance for designing highly selective compounds. Moreover, it remains uncertain whether the covalent adducts of TCP analogs with FAD may induce additional toxicities by influencing the stability or conformation change of the targeted proteins. Modifying the types of covalent adducts formed between TCPs and FAD might also be worth exploring to overcome the toxicity associated with TCPs.

Acknowledgements

This work is supported by the Natural Science Foundation of China (Nos. 32371317, 82473761 and 22277110, china), Natural Science Foundation of Henan Province (Nos. 252300421142, 252300421243 and 242301420005, china), 'Chunhui Plan' Cooperative Scientific Research Project of the Ministry of Education (No. HZKY20220280, china), Key Research Project for Basic Research in Henan Province Universities (No. 25ZX001, china) and Open Research Fund of Key Laboratory of Gastrointestinal Cancer (Fujian Medical University), Ministry of Education (No. FMUGIC-202401, china).

Author contributions

Yihui Song: Writing − original draft. Junbiao Chang: Writing − review & editing. Bin Yu: Writing − review & editing.

Conflicts of interest

The authors declare no conflicts of interest.

References

1. Zhao H, Dietrich J. Privileged scaffolds in lead generation. *Expet Opin Drug Discov* 2015;**10**:781−90.
2. Welsch ME, Snyder SA, Stockwell BR. Privileged scaffolds for library design and drug discovery. *Curr Opin Chem Biol* 2010;**14**: 347−61.
3. Ulrich S, Ricken R, Adli M. Tranylcypromine in mind (Part I): review of pharmacology. *Eur Neuropsychopharmacol* 2017;**27**: 697−713.
4. Frieling H, Bleich S. Tranylcypromine: new perspectives on an "old" drug. *Eur Arch Psychiatr Clin Neurosci* 2006;**256**:268−73.
5. Fang Y, Liao G, Yu B. LSD1/KDM1A inhibitors in clinical trials: advances and prospects. *J Hematol Oncol* 2019;**12**:129.
6. Goel D. Ticagrelor: the first approved reversible oral antiplatelet agent. *Int J Appl Basic Med Res* 2013;**3**:19−21.
7. Tsai TY, Hsu T, Chen CT, Cheng JH, Yeh TK, Chen X, et al. Novel *trans*-2-aryl-cyclopropylamine analogues as potent and selective dipeptidyl peptidase IV inhibitors. *Bioorg Med Chem* 2009;**17**: 2388−99.
8. Chen J, Levant B, Jiang C, Keck TM, Newman AH, Wang S. Tranylcypromine substituted cis-hydroxycyclobutylnaphthamides as potent and selective dopamine D_3 receptor antagonists. *J Med Chem* 2014;**57**:4962−8.
9. Shen HC, Ding FX, Wang S, Deng Q, Zhang X, Chen Y, et al. Discovery of a highly potent, selective, and bioavailable soluble epoxide hydrolase inhibitor with excellent *ex vivo* target engagement. *J Med Chem* 2009;**52**:5009−12.
10. Zhang J, Wang Y, Gao W, Yu B. Progress in the synthesis of 2-phenylcyclopropylamine derivatives. *Chin J Pharm* 2023;**54**:813.
11. Song Y, Zhang H, Yang X, Shi Y, Yu B. Annual review of lysine-specific demethylase 1 (LSD1/KDM1A) inhibitors in 2021. *Eur J Med Chem* 2022;**228**:114042.
12. Li G, Wang Y, De Clercq E. Approved HIV reverse transcriptase inhibitors in the past decade. *Acta Pharm Sin B* 2022;**12**:1567−90.
13. Zeller EA. Amine oxidases. In: Brodie BB, Gillette JR, Ackerman HSeditors, editors. *Concepts in biochemical pharmacology: Part 2*, vol. 28. Berlin Heidelberg: Springer; 1971. p. 518−35.
14. Yang J, Talibov VO, Peintner S, Rhee C, Poongavanam V, Geitmann M, et al. Macrocyclic peptides uncover a novel binding mode for reversible inhibitors of LSD1. *ACS Omega* 2020;**5**: 3979−95.
15. Tararina MA, Allen KN. Bioinformatic analysis of the flavin-dependent amine oxidase superfamily: adaptations for substrate specificity and catalytic diversity. *J Mol Biol* 2020;**432**:3269−88.
16. Vianello P, Botrugno OA, Cappa A, Ciossani G, Dessanti P, Mai A, et al. Synthesis, biological activity and mechanistic insights of 1-substituted cyclopropylamine derivatives: a novel class of irreversible inhibitors of histone demethylase KDM1A. *Eur J Med Chem* 2014;**86**:352−63.
17. Yang M, Culhane JC, Szewczuk LM, Jalili P, Ball HL, Machius M, et al. Structural basis for the inhibition of the LSD1 histone demethylase by the antidepressant *trans*-2-phenylcyclopropylamine. *Biochemistry* 2007;**46**:8058−65.
18. Hattori Y, Matsumoto S, Morimoto S, Daini M, Toyofuku M, Matsuda S, et al. Design, synthesis, and structure−activity relationship of TAK-418 and its derivatives as a novel series of LSD1 inhibitors with lowered risk of hematological side effects. *Eur J Med Chem* 2022;**239**:114522.
19. Mimasu S, Sengoku T, Fukuzawa S, Umehara T, Yokoyama S. Crystal structure of histone demethylase LSD1 and tranylcypromine at 2.25 A. *Biochem Biophys Res Commun* 2008;**366**:15−22.
20. Binda C, Valente S, Romanenghi M, Pilotto S, Cirilli R, Karytinos A, et al. Biochemical, structural, and biological evaluation of tranylcypromine derivatives as inhibitors of histone demethylases LSD1 and LSD2. *J Am Chem Soc* 2010;**132**:6827−33.
21. Li C, Su M, Zhu W, Kan W, Ge T, Xu G, et al. Structure−activity relationship study of indolin-5-yl-cyclopropanamine derivatives as selective lysine specific demethylase 1 (LSD1) inhibitors 2022;**65**: 4335−49.
22. Zheng YC, Yu B, Chen ZS, Liu Y, Liu HM. TCPs: privileged scaffolds for identifying potent LSD1 inhibitors for cancer therapy. *Epigenomics* 2016;**8**:651−66.
23. Malancona S, Altamura S, Filocamo G, Kinzel O, Hernando JI, Rowley M, et al. Identification of MK-5710 ((8a*S*)-8a-methyl-1,3-dioxo-2-[(1*S*, 2*R*)-2-phenylcyclopropyl]-*N*-(1-phenyl-1*H*-pyrazol-5-yl)hexahydroimid azo[1,5-a]pyrazine-7(1*H*)-carboxamide), a potent smoothened antagonist for use in Hedgehog pathway dependent malignancies, part 1. *Bioorg Med Chem Lett* 2011;**21**:4422−8.

24. Bariwal J, Kumar V, Dong Y, Mahato RI. Design of Hedgehog pathway inhibitors for cancer treatment. *Med Res Rev* 2018;**39**: 1137−204.
25. Dai XJ, Liu Y, Xiong XP, Xue LP, Zheng YC, Liu HM. Tranylcypromine based lysine-specific demethylase 1 inhibitor: summary and perspective. *J Med Chem* 2020;**63**:14197−215.
26. Tsukada Y, Fang J, Erdjument-Bromage H, Warren ME, Borchers CH, Tempst P, et al. Histone demethylation by a family of JmjC domain-containing proteins. *Nature* 2006;**439**:811−6.
27. Kaniskan HU, Martini ML, Jin J. Inhibitors of protein methyltransferases and demethylases. *Chem Rev* 2018;**118**:989−1068.
28. Gu F, Lin Y, Wang Z, Wu X, Ye Z, Wang Y, et al. Biological roles of LSD1 beyond its demethylase activity. *Cell Mol Life Sci* 2020;**77**: 3341−50.
29. Wojcieszynska D, Hupert-Kocurek K, Guzik U. Flavin-dependent enzymes in cancer prevention. *Int J Mol Sci* 2012;**13**:16751−68.
30. Fang R, Chen F, Dong Z, Hu D, Barbera Andrew J, Clark Erin A, et al. LSD2/KDM1B and its cofactor NPAC/GLYR1 endow a structural and molecular model for regulation of H3K4 demethylation. *Mol Cell* 2013;**49**:558−70.
31. Li C, Su M, Zhu W, Kan W, Ge T, Xu G, et al. Structure−activity relationship study of indolin-5-yl-cyclopropanamine derivatives as selective lysine specific demethylase 1 (LSD1) inhibitors. *J Med Chem* 2022;**65**:4335−49.
32. Burg JM, Link JE, Morgan BS, Heller FJ, Hargrove AE, McCafferty DG. KDM1 class flavin-dependent protein lysine demethylases. *Biopolymers* 2015;**104**:213−46.
33. Wang X, Huang B, Suzuki T, Liu X, Zhan P. Medicinal chemistry insights in the discovery of novel LSD1 inhibitors. *Epigenomics* 2015;**7**:1379−96.
34. Song Y, Yang X, Yu B. Repurposing antidepressants for anticancer drug discovery. *Drug Discov Today* 2022;**27**:1924−35.
35. Wass M, Gollner S, Besenbeck B, Schlenk RF, Mundmann P, Gothert JR, et al. A proof of concept phase I/II pilot trial of LSD1 inhibition by tranylcypromine combined with ATRA in refractory/relapsed AML patients not eligible for intensive therapy. *Leukemia* 2021;**35**:701−11.
36. Niwa H, Watanabe C, Sato S, Harada T, Watanabe H, Tabusa R, et al. Structure−activity relationship and *in silico* evaluation of *cis*- and *trans*-PCPA-derived inhibitors of LSD1 and LSD2. *ACS Med Chem Lett* 2022;**13**:1485−92.
37. Mimasu S, Umezawa N, Sato S, Higuchi T, Umehara T, Yokoyama S. Structurally designed *trans*-2-phenylcyclopropylamine derivatives potently inhibit histone demethylase LSD1/KDM1. *Biochemistry* 2010;**49**:6494−503.
38. Lee SH, Stubbs M, Liu XM, Diamond M, Dostalik V, Ye M, et al. Abstract 4712: discovery of INCB059872, a novel FAD-directed LSD1 inhibitor that is effective in preclinical models of human and murine AML. *Cancer Res* 2016;**76**:4712.
39. Maes T, Mascaró C, Tirapu I, Estiarte A, Ciceri F, Lunardi S, et al. ORY-1001, a potent and selective covalent KDM1A inhibitor, for the treatment of acute leukemia. *Cancer Cell* 2018;**33**:495−511.e12.
40. Mohammad HP, Smitheman KN, Kamat CD, Soong D, Federowicz KE, Van Aller GS, et al. A DNA hypomethylation signature predicts antitumor activity of LSD1 inhibitors in SCLC. *Cancer Cell* 2015;**28**:57−69.
41. Niwa H, Sato S, Handa N, Sengoku T, Umehara T, Yokoyama S. Development and structural evaluation of *N*-alkylated *trans*-2-phenylcyclopropylamine-based LSD1 inhibitors. *ChemMedChem* 2020;**15**:787−93.
42. Song Y, Wang S, Yu B. Structural and functional landscape of FAD-dependent histone lysine demethylases for new drug discovery. *J Med Chem* 2023;**66**:71−94.
43. Tan AHY, Tu W, McCuaig R, Hardy K, Donovan T, Tsimbalyuk S, et al. Lysine-specific histone demethylase 1A regulates macrophage polarization and checkpoint molecules in the tumor microenvironmol/lent of triple-negative breast cancer. *Front Immunol* 2019;**10**:1351.
44. Ishikawa Y, Gamo K, Yabuki M, Takagi S, Toyoshima K, Nakayama K, et al. A novel LSD1 inhibitor T-3775440 disrupts GFI1B-containing complex leading to transdifferentiation and impaired growth of AML cells. *Mol Cancer Therapeut* 2017;**16**:273−84.
45. Pieroni M, Annunziato G, Azzali E, Dessanti P, Mercurio C, Meroni G, et al. Further insights into the SAR of α-substituted cyclopropylamine derivatives as inhibitors of histone demethylase KDM1A. *Eur J Med Chem* 2015;**92**:377−86.
46. Borrello MT, Schinor B, Bartels K, Benelkebir H, Pereira S, Al-Jamal WT, et al. Fluorinated tranylcypromine analogues as inhibitors of lysine-specific demethylase 1 (LSD1, KDM1A). *Bioorg Med Chem Lett* 2017;**27**:2099−101.
47. Shi Y, Wu YR, Su MB, Shen DH, Gunosewoyo H, Yang F, et al. Novel spirocyclic tranylcypromine derivatives as lysine-specific demethylase 1 (LSD1) inhibitors. *RSC Adv* 2018;**8**:1666−76.
48. Ji YY, Lin SD, Wang YJ, Su MB, Zhang W, Gunosewoyo H, et al. Tying up tranylcypromine: novel selective histone lysine specific demethylase 1 (LSD1) inhibitors. *Eur J Med Chem* 2017;**141**: 101−12.
49. Binda C, Mattevi A, Edmondson DE. Structural properties of human monoamine oxidases A and B. *Int Rev Neurobiol* 2011;**100**:1−11.
50. Högberg M, Sahlberg C, Engelhardt P, Noréen R, Kangasmetsä J, Johansson NG, et al. Urea-PETT compounds as a new class of HIV-1 reverse transcriptase inhibitors. 3. Synthesis and further structure−activity relationship studies of PETT analogues. *J Med Chem* 1999;**42**:4150−60.
51. Tripathi AC, Upadhyay S, Paliwal S, Saraf SK. Privileged scaffolds as MAO inhibitors: retrospect and prospects. *Eur J Med Chem* 2018; **145**:445−97.
52. Bonivento D, Milczek EM, McDonald GR, Binda C, Holt A, Edmondson DE, et al. Potentiation of ligand binding through cooperative effects in monoamine oxidase B. *J Biol Chem* 2010;**285**: 36849−56.
53. Khan MN, Suzuki T, Miyata N. An overview of phenylcyclopropylamine derivatives: biochemical and biological significance and recent developments. *Med Res Rev* 2013;**33**:873−910.
54. Hruschka S, Rosen TC, Yoshida S, Kirk KL, Frohlich R, Wibbeling B, et al. Fluorinated phenylcyclopropylamines. Part 5: effects of electron-withdrawing or -donating aryl substituents on the inhibition of monoamine oxidases A and B by 2-aryl-2-fluorocyclopropylamines. *Bioorg Med Chem* 2008;**16**:7148−66.
55. Yoshida S, Rosen TC, Meyer OG, Sloan MJ, Ye S, Haufe G, et al. Fluorinated phenylcyclopropylamines. Part 3: inhibition of monoamine oxidase A and B. *Bioorg Med Chem* 2004;**12**:2645−52.
56. Ye S, Yoshida S, Frohlich R, Haufe G, Kirk KL. Fluorinated phenylcyclopropylamines. Part 4: effects of aryl substituents and stereochemistry on the inhibition of monoamine oxidases by 1-aryl-2-fluoro-cyclopropylamines. *Bioorg Med Chem* 2005;**13**:2489−99.
57. Finney J, Moon HJ, Ronnebaum T, Lantz M, Mure M. Human copper-dependent amine oxidases. *Arch Biochem Biophys* 2014;**546**: 19−32.
58. Mäki JM. Lysyl oxidases in mammalian development and certain pathological conditions. *Histol Histopathol* 2009;**24**:651−60.
59. Shah MA, Trackman Pc, Fau - Gallop PM, Gallop Pm Fau, Kagan HM, Kagan HM. Reaction of lysyl oxidase with *trans*-2-phenylcyclopropylamine. *J Biol Chem* 1993;**268**:11580−5.
60. Rosen TC, Yoshida S, Fröhlich R, Kirk KL, Haufe G. Fluorinated phenylcyclopropylamines. 2. Effects of aromatic ring substitution and of absolute configuration on inhibition of microbial tyramine oxidase. *J Med Chem* 2004;**47**:5860−71.
61. Hruschka S, Yoshida S, Kirk KL, Haufe G. Fluorinated phenylcyclopropylamines. Part 6: effects of electron withdrawing or donating aryl substituents on the inhibition of tyramine oxidase from Arthrobacter sp. by diastereomeric 2-aryl-2-fluoro-cyclopropylamines. *J Fluor Chem* 2008;**129**:875−80.
62. Yoshida S, Meyer OG, Rosen TC, Haufe G, Ye S, Sloan MJ, et al. Fluorinated phenylcyclopropylamines. 1. Synthesis and effect of

fluorine substitution at the cyclopropane ring on inhibition of microbial tyramine oxidase. *J Med Chem* 2004;**47**:1796−806.
63. Shepard EM, Heggem H, Juda GA, Dooley DM. Inhibition of six copper-containing amine oxidases by the antidepressant drug tranylcypromine. *Biochim Biophys Acta* 2003;**1647**:252−9.
64. Wilmot CM, Saysell CG, Blessington A, Conn DA, Kurtis CR, McPherson MJ, et al. Medical implications from the crystal structure of a copper-containing amine oxidase complexed with the antidepressant drug tranylcypromine. *FEBS (Fed Eur Biochem Soc) Lett* 2004;**576**:301−5.
65. Kinemuchi H. Selective inhibitors of membrane-bound semicarbazide-sensitive amine oxidase (SSAO) activity in mammalian tissues. *Neurotoxicology* 2004;**25**:325−35.
66. Hollebecque A, de Bono JS, Salvagni S, Plummer R, Niccoli P, Capdevila J, et al. 7O updated results from phase I study of CC-90011 in patients (pts) with solid tumours (STs), including neuroendocrine neoplasms (NENs), and relapsed/refractory non-Hodgkin lymphoma (R/R NHL). *Ann Oncol* 2021;**32**:S4.
67. Pankov KV, McArthur AG, Gold DA, Nelson DR, Goldstone JV, Wilson JY. The cytochrome P450 (CYP) superfamily in cnidarians. *Sci Rep* 2021;**11**:9834.
68. Guengerich FP, Waterman MR, Egli M. Recent structural insights into cytochrome P450 function. *Trends Pharmacol Sci* 2016;**37**:625−40.
69. Mast N, Charvet C, Pikuleva IA, Stout CD. Structural basis of drug binding to CYP46A1, an enzyme that controls cholesterol turnover in the brain. *J Biol Chem* 2010;**285**:31783−95.
70. Pikuleva IA, Cartier N. Cholesterol hydroxylating cytochrome P450 46A1: from mechanisms of action to clinical applications. *Front Aging Neurosci* 2021;**13**:696778.
71. Si Z, Guan X, Teng X, Peng X, Wan Z, Li Q, et al. Identification of CYP46A1 as a new regulator of lipid metabolism through CRISPR-based whole-genome screening. *FASEB J* 2020;**34**:13776−91.
72. Cho SA, Rohn-Glowacki KJ, Jarrar YB, Yi M, Kim WY, Shin JG, et al. Analysis of genetic polymorphism and biochemical characterization of a functionally decreased variant in prostacyclin synthase gene (CYP8A1) in humans. *Arch Biochem Biophys* 2015;**569**:10−8.
73. Tanaka D, Tsuda Y, Shiyama T, Nishimura T, Chiyo N, Tominaga Y, et al. A practical use of ligand efficiency indices out of the fragment-based approach: ligand efficiency-guided lead identification of soluble epoxide hydrolase inhibitors. *J Med Chem* 2010;**54**:851−7.
74. Wold EA, Wild CT, Cunningham KA, Zhou J. Targeting the 5-HT2C receptor in biological context and the current state of 5-HT2C receptor ligand development. *Curr Top Med Chem* 2019;**19**:1381−98.
75. Arvidsson LE, Johansson AM, Hacksell U, Nilsson JL, Svensson K, Hjorth S, et al. *N,N*-Dialkylated monophenolic *trans*-2-phenylcyclopropylamines: novel central 5-hydroxytryptamine receptor agonists. *J Med Chem* 1988;**31**:92−9.
76. Vallgårda J, Appelberg U, Arvidsson LE, Hjorth S, Svensson BE, Hacksell U. *trans*-2-aryl-*N,N*-dipropylcyclopropylamines: synthesis and interactions with 5-HT(1A) receptors. *J Med Chem* 1996;**39**:1485−93.
77. Vangveravong S, Kanthasamy A, Lucaites VL, Nelson DL, Nichols DE. Synthesis and serotonin receptor affinities of a series of *trans*-2-(indol-3-yl)cyclopropylamine derivatives. *J Med Chem* 1998;**41**:4995−5001.
78. Pigott A, Frescas S, McCorvy JD, Huang XP, Roth BL, Nichols DE. *trans*-2-(2,5-dimethoxy-4-iodophenyl)cyclopropylamine and *trans*-2-(2,5-dimethoxy-4-bromophenyl)cyclopropylamine as potent agonists for the 5-HT2 receptor family. *Beilstein J Org Chem* 2012;**8**:1705−9.
79. Nichols DE. Structure−activity relationships of serotonin 5-HT2A agonists. *Wiley Interdiscip Rev Membr Transp Signal* 2012;**1**:559−79.
80. Cattaneo M. $P2Y_{12}$ receptors: structure and function. *J Thromb Haemostasis* 2015;**13**:S10−6.
81. Ferri N, Corsini A, Bellosta S. Pharmacology of the new $P2Y_{12}$ receptor inhibitors: insights on pharmacokinetic and pharmacodynamic properties. *Drugs* 2013;**73**:1681−709.
82. Springthorpe B, Bailey A, Barton P, Birkinshaw TN, Bonnert RV, Brown RC, et al. From ATP to AZD6140: the discovery of an orally active reversible $P2Y_{12}$ receptor antagonist for the prevention of thrombosis. *Bioorg Med Chem Lett* 2007;**17**:6013−8.
83. Talele TT. The "Cyclopropyl fragment" is a versatile player that frequently appears in preclinical/clinical drug molecules. *J Med Chem* 2016;**59**:8712−56.
84. Ye H, Chen C, Zhang HC, Haertlein B, Parry TJ, Damiano BP, et al. Carba-nucleosides as potent antagonists of the adenosine 5′-diphosphate (ADP) purinergic receptor $P2Y_{12}$ on human platelets. *ChemMedChem* 2008;**3**:732−6.
85. Fakhrudin N, Pertiwi KK, Takubessi MI, Susiani EF, Nurrochmad A, Widyarini S, et al. A geranylated chalcone with antiplatelet activity from the leaves of breadfruit (Artocarpus altilis). *Pharmacia* 2020;**67**:173−80.
86. Zhang Y. Targeting epidermal growth factor receptor for cancer treatment: abolishing both kinase-dependent and kinase-independent functions of the receptor. *Pharmacol Rev* 2023;**75**:1218−32.
87. Gibson KH, Grundy W, Godfrey AA, Woodburn JR, Ashton SE, Curry BJ, et al. Epidermal growth factor receptor tyrosine kinase: structure−activity relationships and antitumour activity of novel quinazolines. *Bioorg Med Chem Lett* 1997;**7**:2723−8.
88. Pannala M, Kher S, Wilson N, Gaudette J, Sircar I, Zhang SH, et al. Synthesis and structure−activity relationship of 4-(2-aryl-cyclopropylamino)-quinoline-3-carbonitriles as EGFR tyrosine kinase inhibitors. *Bioorg Med Chem Lett* 2007;**17**:5978−82.
89. Gross G, Drescher K. The role of dopamine D3 receptors in antipsychotic activity and cognitive functions. In: Geyer MA, Geditors Gross, editors. *Novel antischizophrenia treatments*, vol. 213. Berlin Heidelberg: Springer; 2012. p. 167−210.
90. Bonifazi A, Saab E, Sanchez J, Nazarova AL, Zaidi SA, Jahan K, et al. Pharmacological and physicochemical properties optimization for dual-target dopamine D_3 (D_3R) and μ-opioid (MOR) receptor ligands as potentially safer analgesics. *J Med Chem* 2023;**66**:10304−41.
91. Wang C, Wu H, Katritch V, Han GW, Huang X-P, Liu W, et al. Structure of the human smoothened receptor bound to an antitumour agent. *Nature* 2013;**497**:338−43.
92. Kinzel O, Alfieri A, Altamura S, Brunetti M, Bufali S, Colaceci F, et al. Identification of MK-5710 ((8a*S*)-8a-methyl-1,3-dioxo-2-[(1*S*, 2*R*)-2-phenylcyclo- propyl]-*N*-(1-phenyl-1*H*-pyrazol-5-yl)hexahydro-imidazo[1,5-a]pyrazine-7(1*H*)-carboxamide), a potent smoothened antagonist for use in Hedgehog pathway dependent malignancies, Part 2. *Bioorg Med Chem Lett* 2011;**21**:4429−35.
93. Malancona S, Altamura S, Filocamo G, Kinzel O, Hernando JIM, Rowley M, et al. Identification of MK-5710 ((8a*S*)-8a-methyl-1,3-dioxo-2-[(1*S*, 2*R*)-2-phenylcyclopropyl]-*N*-(1-phenyl-1*H*-pyrazol-5-yl)hexahydroimid azo[1,5-a]pyrazine-7(1*H*)-carboxamide), a potent smoothened antagonist for use in Hedgehog pathway dependent malignancies, Part 1. *Bioorg Med Chem Lett* 2011;**21**:4422−8.
94. El-Sherbeni AA, El-Kadi AO. The role of epoxide hydrolases in health and disease. *Arch Toxicol* 2014;**88**:2013−32.
95. Imig JD, Hammock BD. Soluble epoxide hydrolase as a therapeutic target for cardiovascular diseases. *Nat Rev Drug Discov* 2009;**8**:794−805.
96. Tanaka D, Tsuda Y, Shiyama T, Nishimura T, Chiyo N, Tominaga Y, et al. A practical use of ligand efficiency indices out of the fragment-based approach: ligand efficiency-guided lead identification of soluble epoxide hydrolase inhibitors. *J Med Chem* 2011;**54**:851−7.
97. Takai K, Nakajima T, Takanashi Y, Sone T, Nariai T, Chiyo N, et al. Structure-based optimization of cyclopropyl urea derivatives as potent soluble epoxide hydrolase inhibitors for potential decrease of renal injury without hypotensive action. *Bioorg Med Chem* 2014;**22**:1548−57.
98. Takai K, Chiyo N, Nakajima T, Nariai T, Ishikawa C, Nakatani S, et al. Three-dimensional rational approach to the discovery of potent

substituted cyclopropyl urea soluble epoxide hydrolase inhibitors. *Bioorg Med Chem Lett* 2015;**25**:1705−8.
99. Zhan P, Pannecouque C, De Clercq E, Liu X. Anti-HIV drug discovery and development: current innovations and future trends. *J Med Chem* 2015;**59**:2849−78.
100. Öberg B. Rational design of polymerase inhibitors as antiviral drugs. *Antivir Res* 2006;**71**:90−5.
101. Fernández-Romero JA, Thorn M, Turville SG, Titchen K, Sudol K, Li J, et al. Carrageenan/MIV-150 (PC-815), a combination microbicide. *Sex Transm Dis* 2007;**34**:9−14.
102. Dighe SN, Collet TA. Recent advances in DNA gyrase-targeted antimicrobial agents. *Eur J Med Chem* 2020;**199**:112326.
103. Mitscher LA, Sharma PN, Chu DT, Shen LL, Pernet AG. Chiral DNA gyrase inhibitors. 1. Synthesis and antimicrobial activity of the enantiomers of 6-fluoro-7-(1-piperazinyl)-1-(2′-*trans*-phenyl-1′-cyclopropyl)-1, 4-dihydro-4-oxoquinoline-3-carboxylic acid. *J Med Chem* 1986;**29**:2044−7.
104. Hunziker D, Hennig M, Peters JU. Inhibitors of dipeptidyl peptidase IV—recent advances and structural views. *Curr Top Med Chem* 2005;**5**:1623−37.